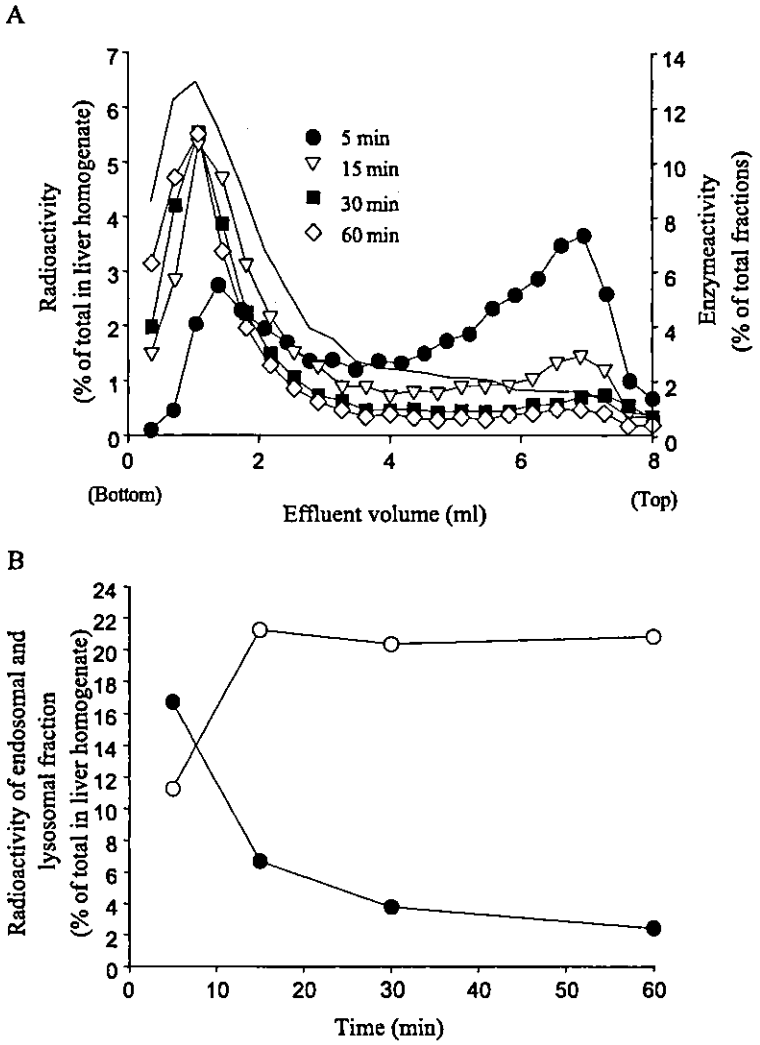

Fig. 5. Each fraction (A) and calculated endosomal (●) or lysosomal (○) localization (B) of radioactivity 5, 15, 30, and 60 min after intravenous administration of [^{111}In]mannosylated bovine serum albumin in mice. Liver homogenate was separated by Percoll density gradient centrifugation. Solid line in A represents the localization of β-hexosamidase activity. Similar results were obtained in two other independent runs.

istration of [^{111}In]lipoplex (B) or Man lipoplex (D). Sixty minutes after intravenous administration, the [^{111}In]Man lipoplex showed a larger distribution to the lysosome fractions than the [^{111}In]lipoplex. For comparison, naked [^{111}In]pDNA, which is extensively accumulated in the liver after intravenous administration but exhibits little gene expression [25], was also subjected to this assay (Fig. 6F). Naked [^{111}In]pDNA showed faster transfer to the lysosome fractions than both the [^{111}In]lipoplex and Man lipoplex.

3.5. PCR amplification

To determine whether pDNA within the subcellular fractions retained its structure, the luciferase sequence of pDNA was amplified by PCR (Fig. 7). When the Man lipoplex was intravenously adminis-

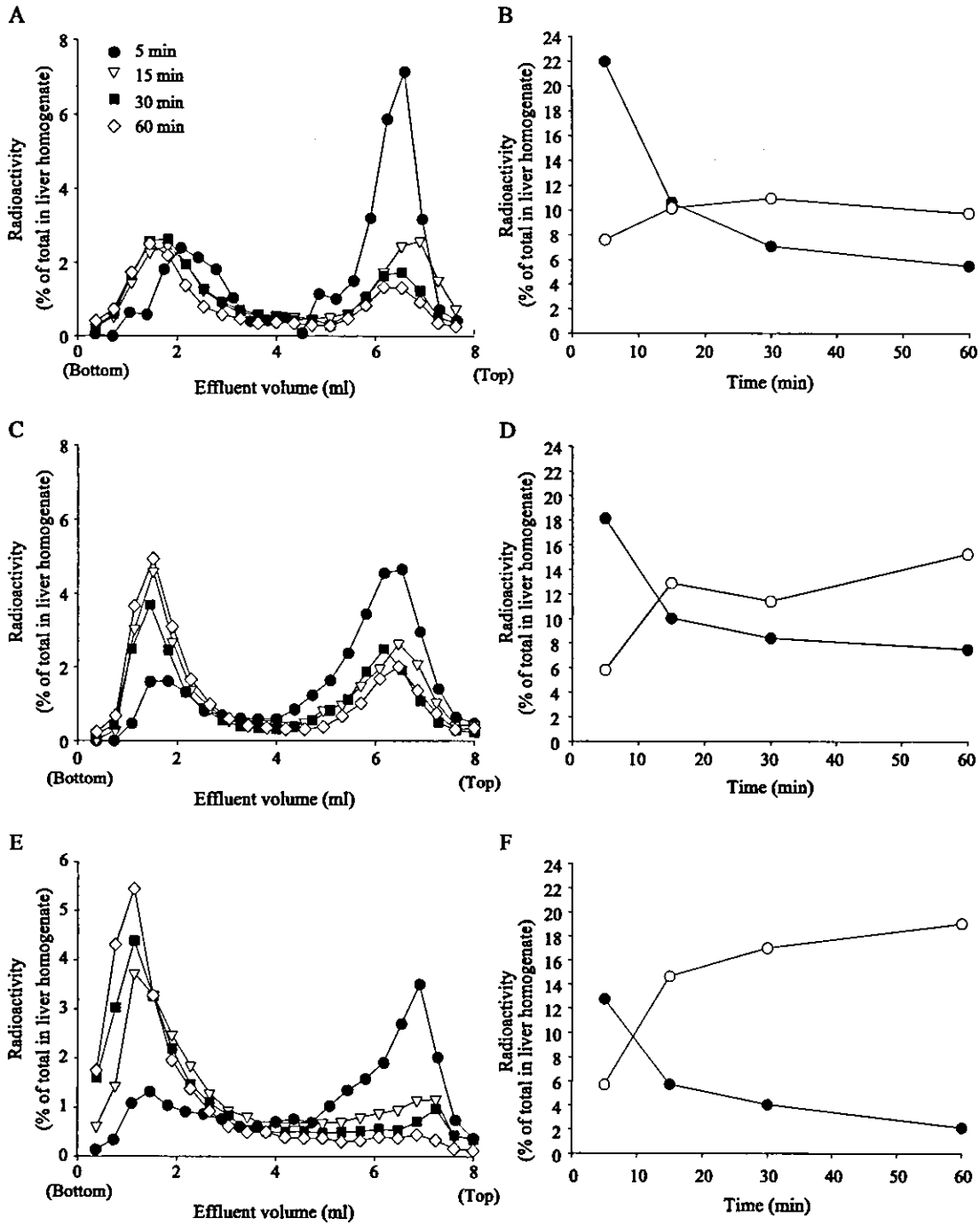

Fig. 6. Each fraction (A, C, and E) and calculated endosomal (●) and lysosomal (○) localization (B, D, and F) of radioactivity 5, 15, 30, and 60 min after intravenous administration of [^{111}In]lipoplex (A, B), Man lipoplex (C, D), or naked [^{111}In]pDNA (E, F) in mice. Liver homogenate was separated by Percoll density gradient centrifugation. Similar results were obtained in two other independent runs.

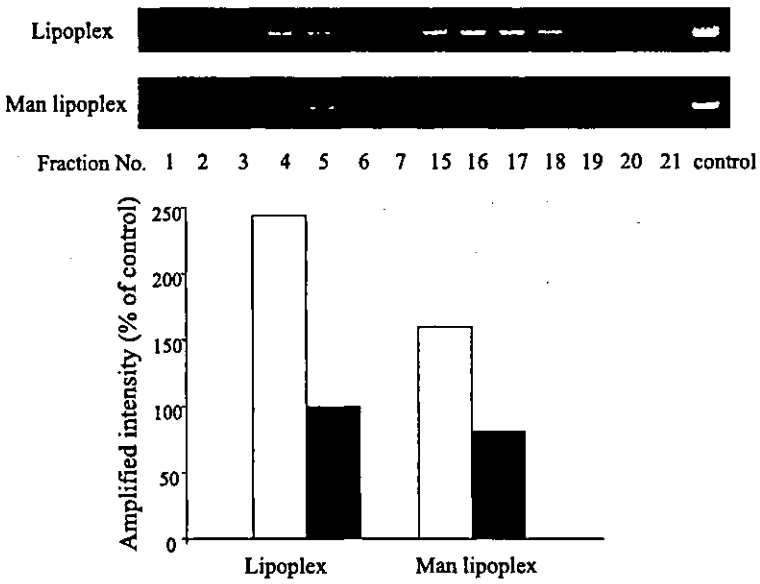

Fig. 7. Amplification of pDNA in endosomal (□) and lysosomal (■) fractions 30 min after intravenous administration of lipoplex and Man lipoplex in mice. Liver homogenate was separated by Percoll density gradient centrifugation. pDNA (1 ng/μl) was used as a control. Similar results were obtained in two other independent runs.

tered, the amounts of DNA amplified from the endosome and lysosome fractions were smaller than those after administration of the lipoplex.

4. Discussion

Transgene expression in target cells after intravenous administration of the Man lipoplex involves a number of distribution processes for pDNA: delivery to the target cells (tissue distribution), internalization, intracellular sorting, and nuclear entry [26]. In particular, the data presented in this study show the importance of intracellular sorting for efficient gene transfection of the Man lipoplex.

Since lipoplex was taken up the cell by the mechanism of endocytosis, pDNA needs to avoid degradation in lysosomes for improving the transfection efficiency. Thus, understanding of the intracellular fate of pDNA will help in the development of better transfection carrier systems. However, there are only a few studies that quantitatively investigate the intracellular fate of pDNA under in vivo conditions. Although so far several tracing methods of pDNA have been used such as ^{32}P-label by nick translation, however, radioactive metabolite, which are generated before and after the cellular uptake of radiolabeled pDNA, often make it extremely difficult to quantitative analyze the tissue distribution and pharmacokinetics of pDNA. In our preliminary experiment, when the fate of internalized [^{32}P]pDNA in liver homogenate was investigated, we found that [^{32}P]pDNA was not suitable for subcellular distribution studies because the radioactivity derived from [^{32}P]pDNA rapidly diminishes due to degradation during the preparation of subcellular fractions. More recently, we have developed [^{111}In]pDNA, an alternative radiolabeling method for pDNA [22], in a similar manner to the preparation of ^{111}In-labeled proteins [27,28], and demonstrated that the radioactivity of [^{111}In]pDNA is slowly released from cells after internalization. Therefore, [^{111}In]pDNA is considered the suitable method for analyzing the tissue and intrahepatic distribution of Man lipoplex. In fact, we observed that both [^{32}P]pDNA and [^{111}In]pDNA mainly accumulated in the liver after intravenous administration, but the radioactivity of ^{32}P gradually decreased (Fig. 2). In contrast, ^{111}In remained at a high level for 2 h after administration (data not shown). Such differences were explained by the poorer membrane permeability

of radioactive metabolites due to the attachment of DTPA for chelation of ^{111}In. Taking this into consideration, [^{111}In]pDNA was effective rebelling method for the subcellular distribution study of lipoplex.

As shown in Fig. 4, the cytoplasmic radioactivity was increased with time after intravenous injection of the [^{111}In]lipoplex and Man lipoplex; accordingly, pDNA is considered to be efficiently released into cytoplasm. On the other hand, the shift of radioactivity from the endosomal to the lysosomal fractions after intravenous administration of the [^{111}In]lipoplex and Man lipoplex suggests that both DC and Man liposomes promote pDNA transfer to lysosomes in the cell (Fig. 6). We previously reported that mannosylated proteins are internalized faster than cationic proteins, which are internalized by the liver via adsorptive endocytosis [16]. Receptor-mediated uptake of the Man lipoplex would explain its faster transport to the lysosome fractions. When naked [^{111}In]pDNA was injected intravenously, however, it showed more rapid transfer to lysosomes than both pDNA complexes. The lysosomes are where internalized substances are degraded, and it can be considered that lysosomal delivery is not suitable for transgene expression. Amplification of pDNA by PCR supported that the Man lipoplex is more rapidly degraded within the intracellular vesicles than the lipoplex (Fig. 7). Therefore, these results suggested that modulation of its intracellular sorting could improve the transfection efficiency of Man lipoplex.

After administration into the blood circulation, the lipoplex interacts with various cells and molecules, such as serum proteins and erythrocytes [29,30]. The cationic nature of the lipoplex attracts negatively charged cells and molecules, which eventually leads to an alteration in the physicochemical properties of the complex. Generally, cellular uptake of a lipoplex is considered to be a nonspecific process based on the interaction of its excess positive charge and the negatively charged cell membrane. Thus, high accumulation of radioactivity was observed both in lung and liver after intravenous administration of the [^{32}P]lipoplex (Fig. 2). On the other hand, the [^{32}P]Man lipoplex did not accumulate in the lung to any great extent compared with the [^{32}P]lipoplex, suggesting that nonspecific interaction could be reduced by mannosylation of cationic liposomes. This distribution study may be partly supported by the fact that our previous observation involved the liver NPC selective gene transfection after intravenous administration of Man lipoplex [10].

In conclusion, the Man lipoplex showed specific accumulation in NPC and achieved higher gene expression than the lipoplex after intravenous administration. It was shown that pDNA delivered by Man liposomes, which is taken up by the mannose receptor, was more susceptible to intracellular degradation than that delivered by conventional cationic liposomes, and this would impair higher gene expression. Also, this observation leads us to believe that further carrier development studies are needed for improving the intracellular sorting of pDNA to avoid degradation.

Acknowledgements

This work was supported in part by Grant-in-Aids for Scientific Research from the Ministry of Education, Culture, Sports, Science, and Technology of Japan, and by Health and Labour Sciences Research Grants for Research on Hepatitis and BSE from the Ministry of Health, Labour and Welfare of Japan.

References

[1] P.L. Felgner, T.R. Gadek, M. Holm, R. Roman, H.W. Chan, M. Wenz, J.P. Northrop, G.M. Ringold, M. Danielsen, Lipofection: a highly efficient, lipid-mediated DNA-transfection procedure, Proc. Natl. Acad. Sci. U. S. A. 84 (1987) 7413–7417.

[2] X. Gao, L. Huang, A novel cationic liposome reagent for efficient transfection of mammalian cells, Biochem. Biophys. Res. Commun. 179 (1991) 280–285.

[3] J.H. Felgner, R. Kumar, C.N. Sridhar, C.J. Wheeler, Y.J. Tsai, R. Border, P. Ramsey, M. Martin, P.L. Felgner, Enhanced gene delivery and mechanism studies with a novel series of cationic lipid formulations, J. Biol. Chem. 269 (1994) 2550–2561.

[4] J.P. Behr, B. Demeneix, J.P. Loeffler, J. Perez-Mutul, Efficient gene transfer into mammalian primary endocrine cells with lipopolyamine-coated DNA, Proc. Natl. Acad. Sci. U. S. A. 86 (1989) 6982–6986.

[5] G.N. Hortobagyi, N.T. Ueno, W. Xia, S. Zhang, J.K. Wolf, J.B. Putnam, P.L. Weiden, J.S. Willey, M. Carey, D.L. Branham, J.Y. Payne, S.D. Tucker, C. Bartholomeusz, R.G. Kilbourn, R.L. De Jager, N. Sneige, R.L. Katz, P. Anklesaria, N.K. Ibrahim, J.L. Murray, R.L. Theriault, V. Valero, D.M. Gershenson, M.W. Bevers, L. Huang, G. Lopez-Berestein, M.C. Hung, Cationic liposome-mediated E1A gene transfer to human breast and ovarian cancer cells and its biologic

effects: a phase I clinical trial, J. Clin. Oncol. 19 (2001) 3422–3433.
[6] S.C. Hyde, K.W. Southern, U. Gileadi, E.M. Fitzjohn, K.A. Mofford, B.E. Waddell, H.C. Gooi, C.A. Goddard, K. Hannavy, S.E. Smyth, J.J. Egan, F.L. Sorgi, L. Huang, A.W. Cuthbert, M.J. Evans, W.H. Colledge, C.F. Higgins, A.K. Webb, D.R. Gill, Repeat administration of DNA/liposomes to the nasal epithelium of patents with cystic fiblosis, Gene Ther. 7 (2000) 1156–1165.
[7] J.S. Remy, A. Kichler, V. Mordvinov, F. Schuber, J.P. Behr, Targeted gene transfer into hepatoma cells with lipopolyamine-condensed DNA particles presenting galactose ligands: a stage toward artificial viruses, Proc. Natl. Acad. Sci. U. S. A. 92 (1995) 1744–1748.
[8] S. Kawakami, F. Yamashita, M. Nishikawa, Y. Takakura, M. Hashida, Asialoglycoprotein receptor-mediated gene transfer using novel galactosylated cationic liposomes, Biochem. Biophys. Res. Commun. 252 (1998) 78–83.
[9] P. Erbacher, M.T. Bousser, J. Raimond, M. Monsigny, P. Midoux, A.C. Roche, Gene transfer by DNA/glycosylated polylysine complex into human blood monocyte-derived macrophages, Hum. Gene Ther. 7 (1996) 721–729.
[10] S. Kawakami, A. Sato, M. Nishikawa, F. Yamashita, M. Hashida, Mannose receptor-mediated gene transfer into macrophages using novel mannosylated cationic liposomes, Gene Ther. 7 (2000) 292–299.
[11] D.T. Curiel, S. Agarwal, M.U. Romer, E. Wagner, M. Cotten, M.L. Birnstiel, R.C. Boucher, Gene transfer to respiratory epithelial cells via the receptor-mediated endocytosis pathway, Am. J. Respir. Cell Mol. Biol. 6 (1992) 247–252.
[12] L. Yano, M. Shimura, M. Taniguchi, Y. Hayashi, T. Suzuki, K. Hatake, F. Takaku, Y. Ishizaka, Improved gene transfer to neuroblastoma cells by a monoclonal antibody targeting RET, a receptor tyrosine kinase, Hum. Gene Ther. 11 (2000) 995–1004.
[13] T. Ohashi, S. Boggs, P. Robbins, A. Bahnson, K. Patrene, F. Wei, J. Wei, J. Li, L. Lucht, Y. Fei, S. Clark, M. Kimak, H. He, P. Mowery-Rushton, J.A. Barranger, Efficient transfer and sustained high expression of the human glucocerebrosidase gene in mice and their functional macrophages following transplantation of bone marrow transduced by a retroviral vector, Proc. Natl. Acad. Sci. U. S. A. 89 (1992) 11332–11336.
[14] D.B. Kohn, N. Sarver, Gene therapy for HIV-1 infection, Adv. Exp. Med. Biol. 394 (1996) 421–428.
[15] S. Kawakami, A. Sato, M. Yamada, F. Yamashita, M. Hashida, The effect of lipid composition on receptor-mediated in vivo gene transfection using mannosylated cationic liposomes in mice, STP Pharma Sci. 11 (2001) 117–120.
[16] K. Ogawara, S. Hasegawa, M. Nishikawa, Y. Takakura, M. Hashida, Pharmacokinetic evaluation of mannosylated bovine serum albumin as a liver cell-specific carrier: quantitative comparison with other hepatotropic ligands, J. Drug Target. 6 (1999) 349–360.
[17] G.R. Bartlett, Phosphorus assay in column chromatography, J. Biol. Chem. 234 (1959) 466–468.
[18] J.Y. Legendre, F.C. Szoka Jr., Cyclic amphipathic peptide–DNA complexes mediate high-efficiency transfection of adherent mammalian cells, Proc. Natl. Acad. Sci. U. S. A. 90 (1993) 893–897.
[19] S. Kawakami, S. Fumoto, M. Nishikawa, F. Yamashita, M. Hashida, In vivo gene delivery to the liver using novel galactosylated cationic liposomes, Pharm. Res. 17 (2000) 306–313.
[20] S. Fumoto, F. Nakadori, S. Kawakami, M. Nishikawa, F. Yamashita, M. Hashida, Analysis of hepatic disposition of galactosylated cationic liposome/plasmid DNA complexes in the rat perfused liver, Pharm. Res. 20 (2003) 1452–1459.
[21] K. Sambrook, E.F. Fritsch, T. Maniatis (Eds.), Molecular Cloning: A Laboratory Manual, 2nd edition, Cold Spring Harbor Laboratory Press, Plainview, NY, 1989.
[22] M. Nishikawa, T. Nakano, T. Okabe, N. Hamaguchi, Y. Yamasaki, Y. Takakura, F. Yamashita, M. Hashida, Residualizing indium-111-radiolabel for plasmid DNA and its application to tissue distribution studies, Bioconjug. Chem. 14 (2003) 955–961.
[23] C.A. Hoppe, Y.C. Lee, The binding and processing of mannose-bovine serum albumin derivatives by rabbit alveolar macrophages, J. Biol. Chem. 258 (1983) 14193–14199.
[24] M.E. Taylor, M.S. Leaning, J.A. Summerfield, Uptake and processing of glycoproteins by rat hepatic mannose receptor, Am. J. Physiol. 252 (1987) E690–E698.
[25] K. Kawabata, Y. Takakura, M. Hashida, The fate of plasmid DNA after intravenous injection in mice: involvement of scavenger receptors in its hepatic uptake, Pharm. Res. 12 (1995) 825–830.
[26] S. Kawakami, F. Yamashita, K. Nishida, J. Nakamura, M. Hashida, Glycosylated cationic liposomes for cell-selective gene delivery, Crit. Rev. Ther. Drug Carr. Syst. 19 (2002) 171–190.
[27] M. Nishikawa, H. Hirabayashi, Y. Takakura, M. Hashida, Design for cell-specific targeting of proteins utilizing sugar-recognition mechanism: effect of molecular weight of proteins on targeting efficiency, Pharm. Res. 12 (1995) 209–214.
[28] Y. Yabe, N. Kobayashi, T. Nishihashi, R. Takahashi, M. Nishikawa, Y. Takakura, M. Hashida, Prevention of neutrophil-mediated hepatic ischemia/reperfusion injury by superoxide dismutase and catalase derivatives, J. Pharmacol. Exp. Ther. 298 (2001) 894–899.
[29] F. Sakurai, T. Nishioka, H. Saito, T. Baba, A. Okuda, O. Matsumoto, T. Taga, F. Yamashita, Y. Takakura, M. Hashida, Interaction between DNA-cationic liposome complexes and erythrocytes is an important factor in systemic gene transfer via the intravenous route in mice: the role of the neutral helper lipid, Gene Ther. 8 (2001) 677–686.
[30] F. Sakurai, T. Nishioka, F. Yamashita, Y. Takakura, M. Hashida, Effects of erythrocytes and serum proteins on lung accumulation of lipoplexes containing cholesterol or DOPE as a helper lipid in the single-pass rat lung perfusion system, Eur. J. Pharm. Biopharm. 52 (2001) 165–172.

Significant Role of Liver Sinusoidal Endothelial Cells in Hepatic Uptake and Degradation of Naked Plasmid DNA After Intravenous Injection

Jin Hisazumi,[1] Naoki Kobayashi,[1] Makiya Nishikawa,[1] and Yoshinobu Takakura[1,2]

Received October 15, 2003; accepted March 14, 2004

Purpose. Uptake and degradation of naked plasmid DNA (pDNA) by liver sinusoidal endothelial cells (LSECs) were investigated.
Methods. Tissue distribution and intrahepatic localization were determined after an intravenous injection of ^{111}In- or ^{32}P-labeled pDNA into rats. Cellular uptake and degradation of fluorescein- or ^{32}P-labeled pDNA were evaluated using primary cultures of rat LSECs.
Results. Following intravenous injection, pDNA was rapidly eliminated from the circulation and taken up by the liver. Fractionation of liver-constituting cells by centrifugal elutriation revealed a major contribution of LSECs to the overall hepatic uptake of pDNA. Confocal microscopic study confirmed intracellular uptake of pDNA in cultured LSECs. Apparent cellular association of pDNA was similar at 37°C and 4°C. However, trichloroacetic acid (TCA) precipitation experiments showed the TCA-soluble radioactivity in the culture medium increased in an accumulative manner at 37°C. Involvement of a specific mechanism was demonstrated, as the uptake of pDNA was significantly inhibited by excess unlabeled pDNA and some polyanions (polyinosinic acid, dextran sulfate, heparin) but not by others (polycytidylic acid, dextran). These inhibitors also reduced the amount of TCA-soluble radioactivity in the culture medium.
Conclusion. These results suggest that LSECs efficiently ingested and rapidly degraded naked pDNA *in vivo* and *in vitro* and released the degradation products into the extracellular space.

KEY WORDS: degradation; liver sinusoidal endothelial cells; plasmid DNA; trichloroacetic acid; uptake.

INTRODUCTION

Plasmid DNA (pDNA), the simplest nonviral vector, is an important macromolecular agent for gene therapy or DNA vaccination (1,2). Though relatively low transfection efficiency is one of the main limiting factors of nonviral gene transfer strategies, pDNA has advantages in terms of its safety and versatility compared with viral vectors that potentially exhibit immunogenicity and undergo mutation thereby reacquiring the ability to produce infection.

In our previous study involving the *in vivo* disposition of pDNA, we demonstrated that pDNA is rapidly removed from the circulation, more quickly than its degradation by nucleases in the blood and other compartments, and taken up by the liver, predominantly by the liver nonparenchymal cells, after intravenous administration to mice (3). We also demonstrated the key role played by liver nonparenchymal cells in the hepatic uptake of pDNA in the single-pass rat liver perfusion system (4). In addition, we found that the hepatic uptake of pDNA involves a specific mechanism similar to, but distinct from, a class A scavenger receptor (SRA), as it was dramatically inhibited by specific polyanions such as polyinosinic acid (poly I) and dextran sulfate but not by polycytidylic acid (poly C) in mice as well as in a rat liver perfusion system; in addition, it was not significantly affected in SRA-knockout mice (3–5). More recently, we suggested that, among the nonparenchymal cells, liver sinusoidal endothelial cells (LSECs), rather than Kupffer cells, made a major contribution to the overall uptake of pDNA, as gadolinium chloride-induced blockade of Kupffer cells did not affect the degree of hepatic uptake of [^{32}P]pDNA in mice (6). However, there has been no direct evidence for the large contribution of LSECs to the hepatic uptake of pDNA.

LSECs are known to play an important role in the induction of immune tolerance (7,8). In addition, the potential capability of LSECs as a major scavenger of circulating DNAs gives rise to the possibility that LSECs participate in the onset of systemic lupus erythematosus, a disease characterized by the production of anti-DNA antibody (9). In order to develop a strategy for optimizing pDNA delivery in gene therapy and DNA vaccination, it is important to elucidate the types of liver cells involved in pDNA uptake because this might be related to pDNA-derived gene expression and pDNA-induced immune responses. In the current study, therefore, we investigated quantitatively the contribution of LSECs to the hepatic uptake of pDNA following intravenous injection in the rat and studied more details of the cellular uptake characteristics of pDNA *in vitro* using primary cultures of rat LSECs.

MATERIALS AND METHODS

Chemicals

[α-^{32}P]dCTP (3000 Ci/mmol) and dextran (MW 70,000) were obtained from Amersham (Buckinghamshire, England). ^{111}Indium chloride was supplied by Nihon Medi-Physics Co. (Takarazuka, Japan). Poly I (MW 103,300) and poly C (MW 99,500) were purchased from Pharmacia (Uppsala, Sweden). Dextran sulfate (MW 150,000) and heparin sodium salt were purchased from Nacalai Tesque (Kyoto, Japan). Type I-A collagenase, dexamethasone, and vascular endothelial growth factor (VEGF) were purchased from Sigma (St. Louis, MO, USA). Type I rat tail collagen and ITS(+) were purchased from BD Biosciences (San Jose, CA, USA). All other chemicals used were of the highest purity available.

Plasmid DNA

pCMV-Luc (10) encoding firefly luciferase was used as a model pDNA throughout the current study. The pDNA amplified in the DH5α strain of *Escherichia coli* was extracted and purified by a QIAGEN Endofree Plasmid Giga Kit (QIAGEN GmvH, Hilden, Germany). The purity was checked by 1% agarose gel electrophoresis followed by ethid-

[1] Department of Biopharmaceutics and Drug Metabolism, Graduate School of Pharmaceutical Sciences, Kyoto University, Kyoto, Japan.
[2] To whom correspondence should be addressed. (e-mail: takakura@pharm.kyoto-u.ac.jp)

ABBREVIATIONS: pDNA, plasmid DNA; poly I, polyinosinic acid; poly C, polycytidylic acid; LSECs, liver sinusoidal endothelial cells; SRA, class A scavenger receptor; TCA, trichloroacetic acid.

0724-8741/04/0700-1223/0 © 2004 Plenum Publishing Corporation

ium bromide staining. The pDNA concentration was measured by UV absorption at 260 nm. For biodistribution or cellular uptake studies, pDNA was radiolabeled with ^{111}In as described below or with [α-^{32}P]dCTP by the nick translation method (11). For confocal microscopic observations, pDNA was labeled with fluorescein using a FastTag FL labeling kit (Vector Laboratories, Burlingame, CA, USA).

Preparation of [^{111}In]pDNA

Radiolabeling of pDNA with ^{111}In was performed by a method described elsewhere (12). Briefly, to a 27.5-μl dimethylsulfoxide solution of 1 mg 4-[*p*-azidosalicylamido]butylamine (ASBA) was added diethylenetriaminepentaacetic acid (DTPA) anhydride (2 mg) under dark-room conditions, and the mixture was incubated at room temperature for 1 h Then, 25 μl pDNA solution (4 mg/ml) was added to the mixture, and the volume was adjusted to 500 μl with phosphate-buffered saline (PBS) of pH 7.4. The mixture was immediately irradiated under a UV lamp (365 nm, UltraViolet Products, Upland, CA, USA) at room temperature for 15 min to obtain DTPA-ASBA coupled pDNA (DTPA-ASBA-pDNA). The product was purified by ethanol precipitation twice and was dissolved in 20 μl acetate buffer (0.1 M, pH 6). To 10 μl sodium acetate solution (1 M) was added 10 μl $^{111}InCl_3$, then 20 μl DTPA-ASBA-pDNA. The mixture was incubated at room temperature for 1 h, and unreacted $^{111}InCl_3$ was removed by ultrafiltration. The purity was checked by Sephadex G-25 column (1 × 40 cm) chromatography and 1% agarose gel electrophoresis.

In Vivo Disposition Studies of pDNA

Male Wistar rats (250 g) were purchased from the Shizuoka Agricultural Co-operate Association for Laboratory Animals (Shizuoka, Japan). All animal experiments were reviewed and approved by the Ethics Committee for Animal Experiments at the Kyoto University.

Rats received [^{32}P]pDNA or [^{111}In]pDNA diluted with unlabeled pDNA (1 mg/kg) in sterilized saline by tail vein injection. The tail vein injection was performed using a 26-gauge needle. Blood was withdrawn from the jugular vein at the indicated times following pDNA injection under anesthesia and then centrifuged to obtain plasma. The rats were euthanized 30 min after urine collection from the urinary bladder, and then the kidney, liver, lung, and heart were excised and rinsed with saline. In the case of [^{32}P]pDNA, the samples of plasma, urine, and small pieces of tissue were dissolved in 0.7 ml Solene-350 at 45°C, followed by the addition of 0.2 ml isopropanol, 0.2 ml H_2O_2, 0.1 ml 5N HCl, and 5 ml Clearsol I (scintillation medium). The radioactivity was measured using a liquid scintillation counter (LSA-500, Beckman, Tokyo, Japan). In the case of [^{111}In]pDNA, the radioactivity of the samples was directly measured in a NaI scintillation counter (ARC-500, Aloka, Tokyo, Japan).

To investigate the intrahepatic distribution of pDNA, rats received [^{111}In]pDNA (1 mg/kg) by tail vein injection under anesthesia. The rats were killed at 30 min, and then the liver was fractionated into parenchymal cells, Kupffer cells, and LSECs as mentioned below. The radioactivity of each cell suspension was measured in a NaI scintillation counter.

Isolation and Culture of Primary LSECs

Isolation of LSECs was performed as previously described (13). Briefly, liver was perfused under anesthesia via the portal vein with Ca^{2+}- and Mg^{2+}-free Hanks' balanced salt solution (HBSS) at 37°C for 10 min at a flow rate of 10–12 ml/min. Then, the liver was perfused with HBSS containing 5 mM Ca^{2+} and 0.05% (w/v) collagenase for 10 min. The digested liver was minced and filtered through a cotton gauze and a nylon mesh (mesh size 45 μm) and then fractionated into hepatocytes and nonparenchymal cells by differential centrifugation. Liver nonparenchymal cells were further separated into LSECs and Kupffer cells by centrifugal elutriation. LSECs were seeded on 24-well plates (1.0×10^6 cells/well), coated beforehand with rat tail collagen, and cultured in RPMI1640 supplemented with 10% fetal calf serum, VEGF (5 μg/ml), ITS(+) (1% v/v), amphotericin B (10 mg/ml), and dexamethasone (0.01 mM) for 4–5 days. The purity of LSECs was checked by immunostaining of factor VIII–related antigen as well as uptake experiment using microparticulates (4.5 μm) and confirmed to be more than 95%. We also ensured the expression of functional receptors on the isolated LSECs in our preliminary *in vitro* uptake experiment using mannosylated BSA (data not shown).

In Vitro Cellular Association Experiments

LSECs were washed three times with 0.5 ml HBSS followed by the addition of 0.5 ml HBSS containing 0.1 μg/ml naked [^{32}P]pDNA. After incubation at 37°C or 4°C for a specified time, incubation medium was removed and the cells were washed five times with ice-cold HBSS and then solubilized with 1.0 ml of 0.3 N NaOH containing 0.1% Triton X-100. Aliquots of the cell lysate were subjected to the determination of ^{32}P radioactivity. To examine the competitive effects of various polyanions on the binding and uptake of pDNA, the described dose of unlabeled pDNA or macromolecules such as poly I, poly C, and dextran sulfate was added to the incubation medium concomitantly with [^{32}P]pDNA.

TCA Precipitation Experiments

To estimate the amount of degradation products of pDNA, following completion of the cellular association experiments, the culture medium and cell lysates were subjected to trichloroacetic acid (TCA) precipitation. After elimination of cellular proteins by extracting with TE buffer-saturated phenol (69% phenol), aliquots of the supernatants and cell lysates were mixed with TCA to give a final concentration of 5% (w/v), kept on ice for 10 min, and then centrifuged at 13,000 rpm for 30 min. The supernatant (TCA-soluble fraction) was subjected to radioactivity measurement. The TCA-soluble fraction is supposed to contain small DNA fragments of degradation products (short oligonucleotides), as longer oligonucleotides (>16-mer) are precipitable in 5% TCA (14).

Confocal Microscopic Study

LSECs cultured on the cover glasses were washed with HBSS and mixed with 5 μg/ml fluorescein-labeled pDNA ([FL]pDNA). After incubation at 37°C or 4°C, the cells were washed and fixed with 4% paraformaldehyde for 1 h. Then, cell sheets were stained with an anti-factor VIII–related an-

tigen mouse IgG (InnoGenex, San Ramon, CA, USA) at 1:200 dilution followed by secondary antibodies, an anti-mouse IgG Alexa Fluor 594 (Molecular Probes, Eugene, OR, USA) at 1:250 dilution. Finally, these samples were subjected to confocal microscopic investigation (MRC-1024, Bio-Rad, Hercules, CA, USA).

RESULTS

In Vivo Disposition of pDNA After Intravenous Injection

First, we examined the *in vivo* disposition of pDNA in rats. Figure 1 shows the time-courses of the plasma concentration of radioactivity and the amounts of radioactivity in the organs and urine at 30 min after intravenous injection of [^{32}P]pDNA or [^{111}In]pDNA (1 mg/kg). pDNA was rapidly eliminated from the circulation and mainly taken up by the liver, similarly to previous studies using mice (3,6). No significant difference was observed, at least during this experimental period, between the radiolabeling methods in terms of the pattern of elimination from plasma and the degree of liver accumulation.

To examine the contribution of liver-constituting cells to the hepatic uptake of pDNA, hepatocytes, LSECs, and Kupffer cells were isolated from the liver following intravenous administration of pDNA. Figure 2 shows the intrahepatic distribution of pDNA at 30 min after intravenous injection of [^{111}In]pDNA at a dose of 1 mg/kg. The amount of pDNA taken up by LSECs and Kupffer cells on a cellular basis (i.e., per 10^8 cells) were significantly greater than that by hepatocytes (Fig. 2A). The relative contributions of hepatocytes, Kupffer cells and LSECs were evaluated on the basis of the numbers of each cell per liver (15,16). As shown in Fig. 2B, pDNA was mostly taken up by LSECs (almost 50% of total hepatic uptake). The estimated total hepatic recovery of injected radioactivity, which was calculated from the data in Fig. 2A on the basis of the number of each cell per 1 g liver assuming the weight of the rat liver to be 8 g, was approximately 70% of the dose, in agreement with the direct measurement of the hepatic accumulation of [^{111}In]pDNA (Fig. 1B). However, in our preliminary study using [^{32}P]pDNA, the

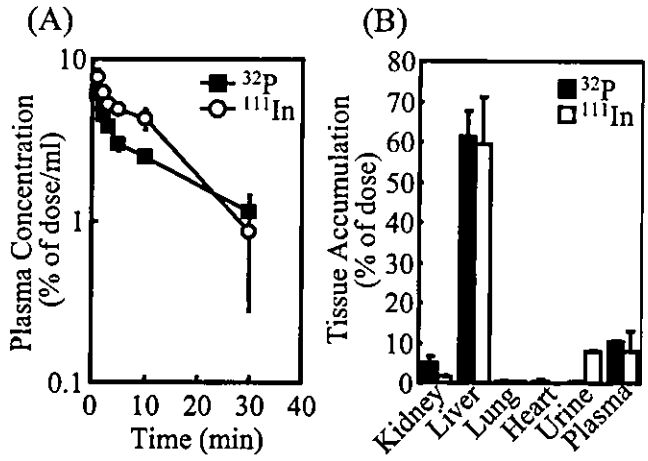

Fig. 1. Time-courses of (A) plasma concentration and (B) tissue accumulation of radioactivity at 30 min after intravenous injection of [^{32}P]pDNA or [^{111}In]pDNA (1 mg/kg) into rats. The results are expressed as mean ± SD (n = 3).

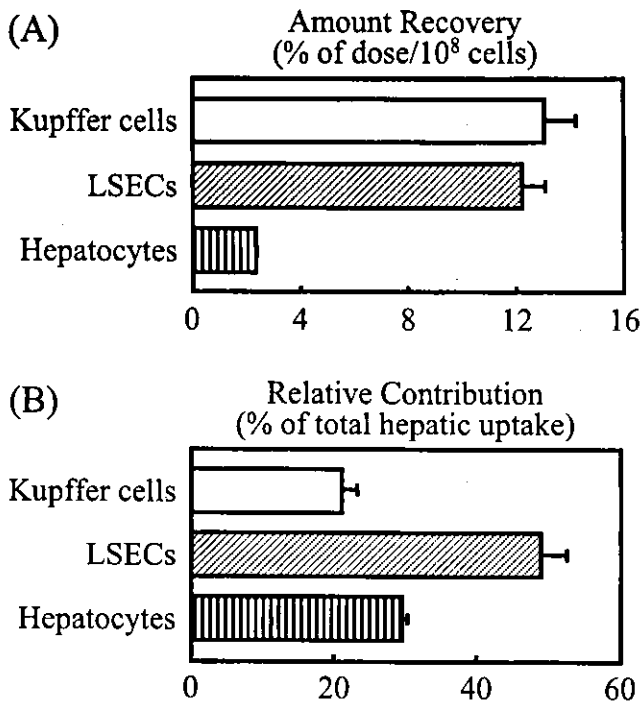

Fig. 2. Intrahepatic distribution of [^{111}In]pDNA (1 mg/kg) on a (A) cellular basis and (B) the relative contribution of each type of liver cell to the total hepatic uptake. Rats were euthanized 30 min after intravenous injection and liver cells were isolated as described in "Materials and Methods." The results are expressed as mean ± SD (n = 3).

estimated liver accumulation following isolation of liver-constituting cells was less than 15% of the dose (data not shown), which was much lower than that determined in Fig. 1B.

Cellular Uptake and Degradation of pDNA in Primary Culture of Rat LSECs

To evaluate the details of the cellular uptake of pDNA by LSECs, *in vitro* studies were performed with primary cultures of rat LSECs. Figure 3 shows the uptake of [FL]pDNA in primary cultures of LSECs assessed by confocal laser scanning microscopy. Fluorescence derived from [FL]pDNA was

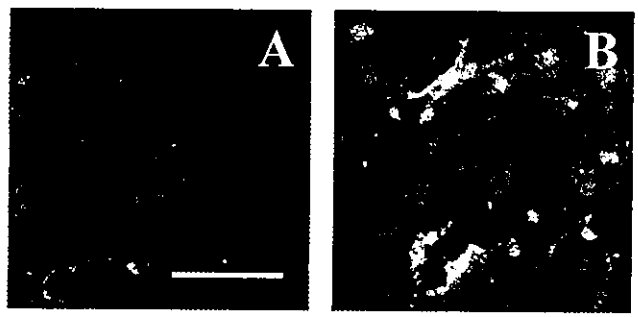

Fig. 3. Confocal microscopic images of LSECs following incubation with [FL]pDNA. The cells were incubated with 0.1 μg/ml [FL]pDNA (green) for 3 h at (A) 4°C or (B) 37°C and fixed with 4% paraformaldehyde and immunostained with anti-factor VIII–related antigen antibody (red). The images shown are typical of those observed in several visual fields. Scale bar represents 50 μm.

restricted to the cell surface or extracellular compartment at 4°C, whereas an intense fluorescence was observed in the intracellular compartment at 37°C.

Figure 4 shows the time-courses of the cellular association and degradation of [^{32}P]pDNA in primary cultures of rat LSECs. The cellular association at 37°C reached a maximum at 1.5 h and then gradually decreased probably due to the release of degradation products into the culture medium. However, at 4°C, a steady increase in the apparent cellular association was observed, although the cells did not appear to internalize pDNA as shown by confocal microscopy. To evaluate the degradation of [^{32}P]pDNA after uptake by LSECs, TCA precipitation experiments were performed. The degradation products of [^{32}P]pDNA in the cellular fraction were at most 2% of the applied dose at 37°C and 4°C (Fig. 4B). On the other hand, a time-dependent dramatic increase was observed in the amount of the degradation products of [^{32}P]pDNA in the culture medium at 37°C, but not at 4°C (Fig. 4C).

Effect of Various Polyanions on Cellular Uptake and Degradation of pDNA in LSECs

We performed competitive studies to examine if the cellular uptake characteristics of pDNA in LSECs were similar to that demonstrated *in vivo* in mice. Figure 5 shows the

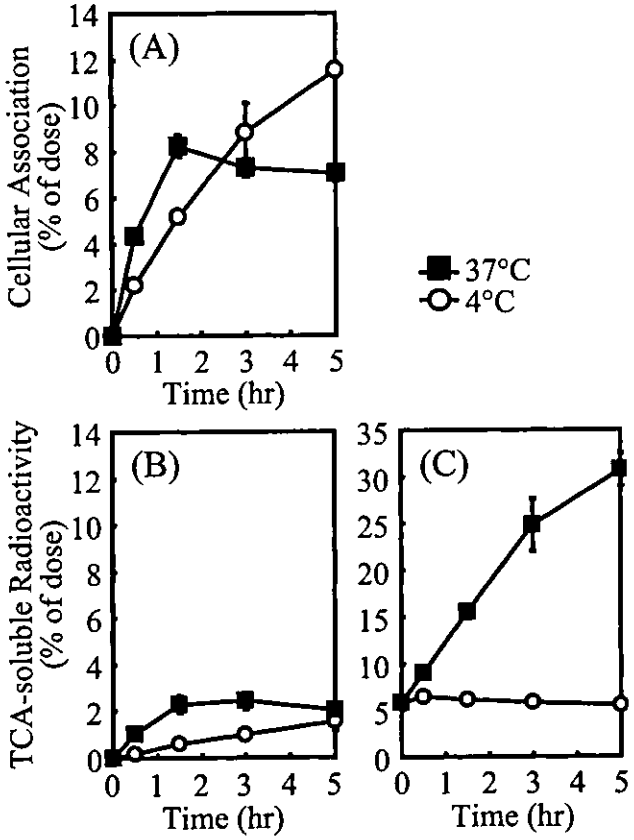

Fig. 4. Time-courses of cellular association of [^{32}P]pDNA with (A) LSECs and TCA-soluble radioactivity in (B) the LSEC cellular fraction and (C) in culture medium. The cells were incubated with [^{32}P]pDNA (0.1 μg/ml) at 37°C (closed square) or 4°C (open circle). Each point represents the mean ± SD (n = 3). The SD was included in the symbol when it was very small.

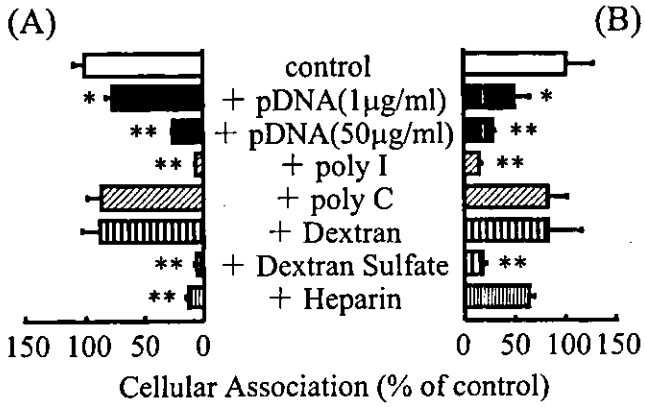

Fig. 5. Competitive effects of various macromolecules on cellular association of [^{32}P]pDNA with LSECs at (A) 4°C or (B) 37°C. The cells were incubated with [^{32}P]pDNA (0.1 μg/ml) for 3 h in the presence or absence of the indicated dose of unlabeled pDNA and various macromolecules (50 μg/ml). The results are expressed as mean ± SD (n = 3). Statistical significance was analyzed by Dunnett's test; $^{**}p < 0.01$, $^{*}p < 0.05$ vs. control.

competitive effects of various macromolecules on the cellular association of [^{32}P]pDNA with LSECs. Excess amounts of unlabeled pDNA inhibited cellular association of [^{32}P]pDNA at 37°C and 4°C. The cellular association was also significantly inhibited by the presence of poly I, dextran sulfate, or heparin, but not by poly C or dextran. To examine further the effect of polyanions on the degradation of [^{32}P]pDNA, the TCA-soluble radioactivity in the culture medium was measured following competitive experiments at 37°C (Fig. 6). Degradation of pDNA was prevented by an excess of unlabeled pDNA and polyanions such as poly I and heparin, which inhibited the cellular association of pDNA.

DISCUSSION

A number of studies involving *in vivo* disposition following intravenous injection of naked DNAs and their complexes, such as single-stranded DNA, double-stranded DNA, oligonucleotide, DNA anti-DNA immune complex, or mononucleosome, have been already reported (17–20). These studies have shown that the liver is the main organ responsible for the rapid clearance of these DNAs from the circulation, while

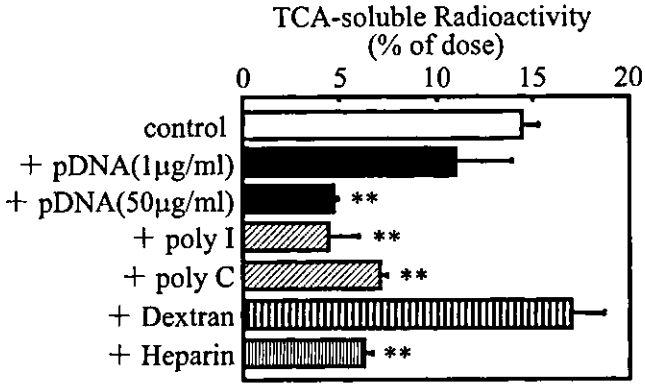

Fig. 6. TCA-soluble radioactivity in the culture medium following competitive experiments at 37°C. The results are expressed as mean ± SD (n = 3). Statistical significance was analyzed by Dunnett's test; $^{**}p < 0.01$ vs. control.

the uptake mechanism and the cell-type(s) contributing to this hepatic uptake remain to be elucidated. We have demonstrated predominant uptake of pDNA by liver nonparenchymal cells (3,4) and suggested the relative importance of LSECs for the overall hepatic uptake of pDNA (6). However, due to lack of direct evidence, more detailed studies need to be performed to confirm the significant contribution of LSECs to pDNA hepatic uptake.

In the current study, we demonstrated efficient uptake and degradation of pDNA by LSECs *in vitro* in primary cell cultures and *in vivo* in rats. We used selective radiolabeling strategies, which allowed us to perform a quantitative analysis of pDNA uptake and degradation. Following intracellular degradation of [^{111}In]pDNA following cellular uptake, ^{111}In should be present as a form of ^{111}In-DTPA-ASBA covalently linked to a single nucleotide or oligonucleotides. Because these metabolites are unlikely to cross biological membranes due to their relatively large size and high hydrophilicity, the ^{111}In-radioactivity could remain within the cells, as is the case of ^{111}In-DTPA-lysine for ^{111}In-labeled protein (21). Therefore, we used [^{111}In]pDNA for the quantitative study of the intrahepatic distribution of pDNA (Fig. 2), expecting a stable retention of the intracellular radioactivity during the isolation steps. Indeed, the intracellular ^{32}P-radioactivity was substantially reduced after the isolation steps (data not shown). However, the amount of degradation product of pDNA could not be determined with [^{111}In]pDNA because [^{111}In]pDNA is unsuitable for the TCA precipitation method. Therefore, [^{32}P]pDNA was used for the *in vitro* experiments involving cellular association and degradation of pDNA (Figs. 4–6) in order to estimate the amount of extracellular or intracellular degradation products by the TCA precipitation method.

We first examined the *in vivo* disposition of pDNA in rats and showed that pDNA was rapidly eliminated from the circulation and taken up by the liver after intravenous injection (Fig. 1), similarly to our previous findings using mice (3,6). A quantitative analysis of the intrahepatic distribution of [^{111}In]pDNA revealed that the amount of radioactivity taken up by LSECs and Kupffer cells, being much higher than those recovered in hepatocytes, was similar in cell number basis, thereby indicating a large contribution of LSECs to the overall hepatic uptake of pDNA following intravenous injection (Fig. 2), as the liver contains 2.5-fold more LSECs than Kupffer cells (15,16). This supports the fact that inhibition of Kupffer cells by gadolinium chloride did not significantly reduce the total hepatic uptake of [^{32}P]pDNA in mice (6). Taken together, the current findings imply a significant role of LSECs in pDNA clearance, in addition to the previous suggestion that the hepatic uptake of intravenously injected pDNA is largely mediated by Kupffer cells (22).

In uptake experiments with primary cultures of LSECs, the degree of the apparent cellular association of [^{32}P]pDNA was similar at 37°C and 4°C (Fig. 4A), although internalization of [FL]pDNA was observed at 37°C but not at 4°C (Fig. 3). The amount of degradation products of [^{32}P]pDNA in the cellular compartment increased rapidly at 37°C, while it was a small fraction of the applied radioactivity, suggesting that rapid degradation of pDNA occurred in LSECs. At the same time, a dramatic increase in the degradation products of [^{32}P]pDNA in the culture medium was observed at 37°C, whereas there was no increase in radioactivity at 4°C (Fig. 4C). These results suggested that pDNA was internalized and rapidly degraded by LSECs and that degraded fragments of pDNA were readily released into the culture medium. The degradation of [^{32}P]pDNA observed in the current study seems to occur predominantly in the intracellular compartment following internalization or on the surface of the LSECs, but not in the culture medium, as no significant degradation was observed during incubation of [^{32}P]pDNA with medium alone, which had been exposed to LSECs for 3 h (data not shown).

A specific mechanism is involved in the cellular uptake process of pDNA by LSECs as shown in the competitive experiment. pDNA uptake and binding were significantly inhibited by excess unlabeled pDNA and some polyanions such as poly I, dextran sulfate, or heparin, but not by others such as poly C or dextran (Fig. 5). This inhibition pattern highly resembles that of our previous *in vivo* study using mice (6), supporting the hypothesis that LSECs make a major contribution to the hepatic uptake of intravenously injected pDNA. Poly I but not poly C is known to form a base quartet-stabilized four strand helix (quadruplex) (23). This hyperstructure would be highly polyanionic. Similar speculation could be applied to polysaccharides such as dextran sulfate and heparin, because they are also highly sulfated. LSECs express various types of receptors essential for endocytosis, such as mannose receptors (24), Fcγ receptors (25), and various classes of scavenger receptors such as SRA, CD36 (class B), LOX-1 (class E), and SREC (class F) (26). Although we could not conclude at this moment which uptake pathway or receptors are involved in pDNA recognition, the results of competitive inhibition experiments have led to the hypothesis that putative receptor(s) on LSECs might recognize pDNA based on its highly polyanionic nature. We have demonstrated that pDNA is taken up by cultured macrophages (27), dendritic cells (28), and brain microvessel endothelial cells (29) via a specific mechanism resembling scavenger receptors. In addition, class A scavenger receptors (SRA) that recognize a wide variety of anionic macromolecules are unlikely to be responsible for pDNA uptake as shown by *in vivo* and *in vitro* experiments using SRA-knockout mice and peritoneal macrophages from these animals (5). Because the inhibition pattern of pDNA uptake is very similar in those different cell types, the cellular uptake mechanisms might be highly conserved among cells including LSECs. It might not be excluded for *in vivo* situation that the serum cationic proteins or complement proteins interact with circulating pDNA and this could facilitate the recognition and uptake of pDNA by LSECs. However, in our previous study using rat liver perfusion system, pDNA was taken up by the liver nonparenchymal cells in the absence of serum via a similar mechanisms involved *in vivo* following intravenous injection. Because serum-free HBSS was used in the current *in vitro* study to avoid serum nuclease-mediated pDNA degradation before recognition by LSECs, the observed pDNA uptake by LSECs was not dependent on these serum proteins. Though further studies are required to elucidate the mechanism involved in pDNA uptake by LSECs, the high density of negative charges arising from the phosphate groups of pDNA may be an important factor.

It is also suggested that pDNA taken up by LSECs is susceptible to degradation. It is likely that the degradation occurs enzymatically predominantly inside the cells probably by DNase II in lysosomes (30) following internalization via

endocytosis, although degradation on the surface of the cells by membrane-bound DNase is not excluded (22). In fact, the degradation was strongly inhibited by cellular uptake inhibitors (Fig. 6), suggesting that the uptake of pDNA by LSECs via the specific mechanism seems to be indispensable for pDNA degradation. This implies that the specific uptake is associated with the pDNA degradation in the LSECs. Unexpectedly, the degradation of pDNA appeared to be inhibited by poly C. Although poly C showed no inhibitory effect on pDNA uptake and binding (Fig. 5), it might affect pDNA degradation in a nonspecific manner.

In conclusion, the current study has shown that LSECs, as well as Kupffer cells, play a key role in the clearance of circulating pDNA following intravenous injection, providing a larger contribution to the overall hepatic uptake of pDNA. We have demonstrated that naked pDNA is efficiently taken up via a specific mechanism and rapidly degraded by LSECs, the degradation products being released into the extracellular space. These findings provide useful information for pDNA delivery in gene therapy and DNA vaccination procedures.

ACKNOWLEDGMENTS

This work was supported, in part, by a grant-in-aid for Scientific Research from the Ministry of Education, Culture, Sports, Science and Technology, Japan.

REFERENCES

1. M. Nishikawa and L. Huang. Nonviral vectors in the new millennium: delivery barriers in gene transfer. *Hum. Gene Ther.* **12**:861–870 (2001).
2. N. Kobayashi, M. Nishikawa, and Y. Takakura. Gene therapy and gene delivery. In B. Wang, T. Siahaan, and R. Soltero (eds.), *Delivery Issues in Drug Discovery*, in press.
3. K. Kawabata, Y. Takakura, and M. Hashida. The fate of plasmid DNA after intravenous injection in mice: involvement of scavenger receptors in its hepatic uptake. *Pharm. Res.* **12**:825–830 (1995).
4. M. Yoshida, R. I. Mahato, K. Kawabata, Y. Takakura, and M. Hashida. Disposition characteristics of plasmid DNA in the single-pass rat liver perfusion system. *Pharm. Res.* **13**:599–603 (1996).
5. Y. Takakura, T. Takagi, M. Hashiguchi, M. Nishikawa, F. Yamashita, T. Doi, T. Imanishi, H. Suzuki, T. Kodama, and M. Hashida. Characterization of plasmid DNA binding and uptake by peritoneal macrophages from class A scavenger receptor knockout mice. *Pharm. Res.* **16**:503–508 (1999).
6. N. Kobayashi, T. Kuramoto, K. Yamaoka, M. Hashida, and Y. Takakura. Hepatic uptake and gene expression mechanisms following intravenous administration of plasmid DNA by conventional and hydrodynamics-based procedures. *J. Pharmacol. Exp. Ther.* **297**:853–860 (2001).
7. P. A. Knolle and G. Gerken. Local control of the immune response in the liver. *Immunol. Rev.* **174**:21–34 (2000).
8. A. Limmer, J. Ohl, C. Kurts, H. G. Ljunggren, Y. Reiss, M. Groettrup, F. Momburg, B. Arnold, and P. A. Knolle. Efficient presentation of exogenous antigen by liver endothelial cells to CD8+ T cells results in antigen-specific T-cell tolerance. *Nat. Med.* **6**:1348–1354 (2000).
9. D. S. Pisetsky. Anti-DNA and autoantibodies. *Curr. Opin. Rheumatol.* **12**:364–368 (2000).
10. T. Nomura, K. Yasuda, T. Yamada, S. Okamoto, R. I. Mahato, Y. Watanabe, Y. Takakura, and M. Hashida. Gene expression and antitumor effects following direct interferon (IFN)-gamma gene transfer with naked plasmid DNA and DC-chol liposome complexes in mice. *Gene Ther.* **6**:121–129 (1999).
11. J. Sambrook, E. F. Fritsch, and T. Maniatis. *Molecular Cloning*, Cold Spring Harbor Laboratory, Cold Spring Harbor, New York, 1989.
12. M. Nishikawa, T. Nakano, T. Okabe, N. Hamaguchi, Y. Yamasaki, Y. Takakura, F. Yamashita, and M. Hashida. Residualizing indium-111-radiolabel for plasmid DNA and its application to tissue distribution study. *Bioconjug. Chem.* **14**:955–961 (2003).
13. J. F. Nagelkerke, K. P. Barto, and T. J. van Berkel. In vivo and in vitro uptake and degradation of acetylated low density lipoprotein by rat liver endothelial, Kupffer, and parenchymal cells. *J. Biol. Chem.* **258**:12221–12227 (1983).
14. J. E. Cleaver and H. W. Boyer. Solubility and dialysis limits of DNA oligonucleotides. *Biochim. Biophys. Acta* **262**:116–124 (1972).
15. R. Blomhoff, H. K. Blomhoff, H. Tolleshaug, T. B. Christensen, and T. Berg. Uptake and degradation of bovine testes beta-galactosidase by parenchymal and nonparenchymal rat liver cells. *Int. J. Biochem.* **17**:1321–1328 (1985).
16. S. Magnusson and T. Berg. Endocytosis of ricin by rat liver cells in vivo and in vitro is mainly mediated by mannose receptors on sinusoidal endothelial cells. *Biochem. J.* **291**:749–755 (1993).
17. W. Emlen and M. Mannik. Effect of DNA size and strandedness on the in vivo clearance and organ localization of DNA. *Clin. Exp. Immunol.* **56**:185–192 (1984).
18. W. Emlen and G. Burdick. Clearance and organ localization of small DNA anti-DNA immune complexes in mice. *J. Immunol.* **140**:1816–1822 (1988).
19. V. J. Gauthier, L. N. Tyler, and M. Mannik. Blood clearance kinetics and liver uptake of mononucleosomes in mice. *J. Immunol.* **156**:1151–1156 (1996).
20. W. Emlen and M. Mannik. Kinetics and mechanisms for removal of circulating single-stranded DNA in mice. *J. Exp. Med.* **147**: 684–699 (1978).
21. F. N. Franano, W. B. Edwards, M. J. Welch, and J. R. Duncan. Metabolism of receptor targeted 111In-DTPA-glycoproteins: identification of 111In-DTPA-epsilon-lysine as the primary metabolic and excretory product. *Nucl. Med. Biol.* **21**:1023–1034 (1994).
22. W. Emlen, A. Rifai, D. Magilavy, and M. Mannik. Hepatic binding of DNA is mediated by a receptor on nonparenchymal cells. *Am. J. Pathol.* **133**:54–60 (1988).
23. A. M. Pearson, A. Rich, and M. Krieger. Polynucleotide binding to macrophage scavenger receptors depends on the formation of base-quartet-stabilized four-stranded helices. *J. Biol. Chem.* **268**: 3546–3554 (1993).
24. A. L. Hubbard, G. Wilson, G. Ashwell, and H. Stukenbrok. An electron microscope autoradiographic study of the carbohydrate recognition systems in rat liver. I. Distribution of 125I-ligands among the liver cell types. *J. Cell Biol.* **83**:47–64 (1979).
25. H. Muro, H. Shirasawa, M. Maeda, and S. Nakamura. Fc receptors of liver sinusoidal endothelium in normal rats and humans. A histologic study with soluble immune complexes. *Gastroenterology* **93**:1078–1085 (1987).
26. V. Terpstra, E. S. van Amersfoort, A. G. van Velzen, J. Kuiper, and T. J. van Berkel. Hepatic and extrahepatic scavenger receptors: function in relation to disease. *Arterioscler. Thromb. Vasc. Biol.* **20**:1860–1872 (2000).
27. T. Takagi, M. Hashiguchi, R. I. Mahato, H. Tokuda, Y. Takakura, and M. Hashida. Involvement of specific mechanism in plasmid DNA uptake by mouse peritoneal macrophages. *Biochem. Biophys. Res. Commun.* **245**:729–733 (1998).
28. T. Yoshinaga, K. Yasuda, Y. Ogawa, and Y. Takakura. Efficient uptake and rapid degradation of plasmid DNA by murine dendritic cells via a specific mechanism. *Biochem. Biophys. Res. Commun.* **299**:389–394 (2002).
29. M. Nakamura, P. Davila-Zavala, H. Tokuda, Y. Takakura, and M. Hashida. Uptake and gene expression of naked plasmid DNA in cultured brain microvessel endothelial cells. *Biochem. Biophys. Res. Commun.* **245**:235–239 (1998).
30. C. Odaka and T. Mizuochi. Role of macrophage lysosomal enzymes in the degradation of nucleosomes of apoptotic cells. *J. Immunol.* **163**:5346–5352 (1999).

THE JOURNAL OF GENE MEDICINE
J Gene Med 2004; 6: 584–592.
Published online 18 February 2004 in Wiley InterScience (www.interscience.wiley.com). DOI: 10.1002/jgm.541

RESEARCH ARTICLE

Hydrodynamics-based procedure involves transient hyperpermeability in the hepatic cellular membrane: implication of a nonspecific process in efficient intracellular gene delivery

Naoki Kobayashi
Makiya Nishikawa
Kazuhiro Hirata
Yoshinobu Takakura*

Department of Biopharmaceutics and Drug Metabolism, Graduate School of Pharmaceutical Sciences, Kyoto University, Sakyo-ku, Kyoto 606-8501, Japan

*Correspondence to:
Yoshinobu Takakura, Department of Biopharmaceutics and Drug Metabolism, Graduate School of Pharmaceutical Sciences, Kyoto University, Sakyo-ku, Kyoto 606-8501, Japan.
E-mail:
takakura@pharm.kyoto-u.ac.jp

Received: 5 September 2003
Revised: 5 December 2003
Accepted: 16 December 2003

Abstract

Background The mechanisms underlying the efficient gene transfer by a large-volume and high-speed intravenous injection of naked plasmid DNA (pDNA), a so-called hydrodynamics-based procedure, remain unclear and require further investigation. In this report, we have investigated possible mechanisms for the intracellular transport of naked pDNA by this procedure.

Methods Propidium iodide (PI), a fluorescent indicator for cell membrane integrity, and luciferase- or green fluorescent protein (GFP)-expressing pDNA were injected into mice by the hydrodynamics-based procedure.

Results PI was efficiently taken up by hepatocytes which appeared to be viable following the hydrodynamics-based procedure. Pre-expressed GFP in the cytosol was rapidly eliminated from the hepatocytes by a large-volume injection of saline. The profiles of plasma ALT and AST showed a steady decline with the highest values observed immediately after the hydrodynamics-based procedure. These results suggest that the hydrodynamics-based procedure produces a transient increase in the permeability of the cell membrane. The cellular uptake process appeared nonspecific, since simultaneous injection of an excess of empty vector did not affect the transgene expression. Sequential injections of a large volume of pDNA-free saline followed by naked pDNA in a normal volume revealed that the increase in membrane permeability was transient, with a return to normal conditions within 30 min. Transgene expression was observed in hepatocyte cultures isolated 10 min after pDNA delivery and in the liver as early as 10 min after luciferase-expressing RNA delivery, indicating that pDNA delivered immediately by the hydrodynamics-based procedure has the potential to produce successful transgene expression.

Conclusions These findings suggest that the mechanism for the hydrodynamics-based gene transfer would involve in part the direct cytosolic delivery of pDNA through the cell membrane due to transiently increased permeability. Copyright © 2004 John Wiley & Sons, Ltd.

Keywords hydrodynamics-based procedure; plasmid DNA; membrane permeability; gene delivery

Introduction

Nonviral gene delivery, which represents a promising *in vivo* gene transfer strategy due to its safety and versatility, has problems associated with the limited efficacy of transgene expression. Various physical or chemical approaches, such as electroporation, gene gun, and complex formation with cationic lipids or polymers, have been studied and developed to improve transgene expression efficacy and the target cell specificity of plasmid DNA (pDNA)-based nonviral gene transfer [1,2]. While these approaches have resulted in a relatively improved efficacy, current nonviral gene delivery systems are likely to require further improvements before their successful application to clinical gene therapy.

Hydrodynamics-based gene delivery, involving a large-volume and high-speed intravenous injection of naked pDNA, gives a significantly high level of transgene expression in the liver and other major organs [3,4]. This procedure has been used very frequently as a simple and convenient *in vivo* transfection method [5–17]. Furthermore, this method of gene transfer allows naked pDNA to be sufficiently effective to obtain therapeutic levels of target transgene products [6,9,10,15–17]. The principle of the hydrodynamics-based procedure could be applicable to an organ-restricted gene delivery method; i.e. targeting to the organs such as the liver, the kidney and the hindlimb muscles by injection via a suitable vein or artery with transient occlusion of the outflow as demonstrated previously [18–23]. In actual fact, Eastman *et al.* [24] recently reported the catheter-mediated hydrodynamics-based delivery of pDNA using isolated rabbit liver.

In spite of the frequent use of the hydrodynamics-based procedure in functional studies of therapeutic genes or DNA elements, little is known about the mechanisms underlying efficient gene transfer by this procedure. Liu *et al.* [3] demonstrated that a rapid injection and a large volume of pDNA solution were required to obtain a high level of transgene expression, indicating that a high blood pressure was the most critical factor for the gene transfer efficiency, and proposed that pDNA might be transferred inside the liver cells by the 'hydrodynamic' process. In contrast, it was hypothesized that the cellular uptake mechanism of naked pDNA injected by the hydrodynamics-based procedure involved a specific process such as receptor-mediated endocytosis [25]. In our previous study, involving the *in vivo* disposition of naked pDNA following the normal or the hydrodynamics-based procedure, in support of the speculation of Liu and colleagues, we demonstrated that the hepatic uptake process appeared nonspecific, being different from that involved in the normal intravenous injection of naked pDNA [26]. Since the cellular uptake mechanisms are still controversial, they need to be better understood for further application of the hydrodynamics-based procedure for both therapeutic applications and basic studies. In the present study, we have investigated a possible mechanism for hydrodynamics-based gene transfer and suggest that it would involve in part a nonspecific process via a cell membrane which becomes permeable for a short period.

Materials and methods

Chemicals

Propidium iodide (PI), type I-A collagenase, type II-S soybean trypsin inhibitor, and William's medium E were purchased from Sigma (St. Louis, MO, USA). Type I rat tail collagen and ITS(+) were purchased from BD Biosciences (San Jose, CA, USA). Injectable saline solution purchased from Otsuka (Tokyo, Japan) was used as the vehicle for plasmid DNA (pDNA) or PI injection in all the experiments. All other chemicals used were of the highest purity available.

Plasmid DNA

pEGFP-N1 encoding enhanced green fluorescent protein (EGFP) and pEGFP-F encoding farnesylated EGFP, that remain bounds to the plasma membrane in both living and fixed cells [27,28], were purchased from BD Biosciences Clontech (Palo Alto, CA, USA). pcDNA3 vector was purchased from Invitrogen (Carlsbad, CA, USA). pCMV-Luc was constructed by insertion of the Hind III/Xba I firefly luciferase cDNA fragment from pGL3-control (Promega, Madison, WI, USA) into the polylinker of pcDNA3 as described earlier [29]. pRLIL-3'NC containing sea pansy luciferase and firefly luciferase genes was kindly provided by Professor Kunitada Shimotohno (Department of Viral Oncology, Institute for Virus Research, Kyoto University, Japan). Each pDNA was amplified in the DH5α strain of *Escherichia coli* and purified using a QIAGEN Endofree Plasmid Giga kit (QIAGEN GmbH, Hilden, Germany).

RNA synthesis

Luciferase-expressing RNA was synthesized by *in vitro* transcription using a MEGAscript T7 kit (Ambion, Austin, TX, USA) according to the manufacturer's instructions. Hind III-linearized pRLIL-3'NC was used as a template. The transcribed RNA was treated with DNase I to minimize template contamination and purified by a standard phenol/chloroform extraction and isopropanol precipitation method. Since no cap analogs were added to the reaction mixture, the transcribed RNA could produce only the internal ribosomal entry site (IRES)-dependent expression of firefly luciferase. The synthesized RNA was dissolved in saline (Otsuka) just before intravenous injection to mice.

J Gene Med 2004; 6: 584–592.

Mice and intravenous injection

Four-week-old female ddY mice (approximately 20 g body weight), purchased from Shizuoka Agricultural Cooperative Association for Laboratory Animals (Shizuoka, Japan), were used for all experiments. Mice received a tail vein injection in a volume of 100 μl (otherwise mentioned) or 1.6 ml for the normal or the hydrodynamics-based procedure, respectively. The tail vein injection was performed over less than 5 s using a 26-gauge needle for both procedures.

Confocal microscopic study of liver sections

Mice were euthanized by cutting the vena cava at the described time and the liver was gently infused with 5 ml saline through the portal vein to remove remaining blood. The liver was then embedded in Tissue-Tek OCT embedding compound (Sakura Finetechnical Co., Ltd., Tokyo, Japan), frozen in liquid nitrogen and stored in 2-methylbutanol at −80 °C. Frozen liver sections were made, 8 μm in thickness, using a cryostat (Jung Frigocut 2800E; Leica Microsystems AG, Wetzlar, Germany) by the routine procedure. With some exceptions, the sections were directly subjected to confocal microscopic observation (MRC-1024; BioRad, Hercules, CA, USA) without any fixation, since the fixation step caused a massive loss of GFP due to immediate dissolution in the fixation buffer in our preliminary experiments. In the case of mice injected with PI alone, their liver sections were fixed with Mildform 20N (8% paraformaldehyde; Wako, Osaka, Japan) for 4 min at 4 °C followed by confocal microscopic observation.

Luciferase assay

To determine luciferase activities, the organs including the liver, kidney, lung, spleen and heart were excised and homogenized in 5 ml/g (liver) or 4 ml/g (other organs) of lysis buffer (0.1 M Tris, 0.05% Triton X-100, 2 mM EDTA, pH 7.8). The homogenate was subjected to three cycles of freezing (−190 °C) and thawing (37 °C) and centrifuged at 10 000 g for 10 min at 4 °C. Then, appropriately diluted supernatant was mixed with luciferase assay buffer (Picagene, Toyo Ink, Tokyo, Japan) and the chemiluminescence produced was measured in a luminometer (Lumat LB 9507; EG & G Berthold, Bad Wildbad, Germany).

Determination of plasma transaminase activities

At the indicated time points after large-volume injection of saline, blood was collected from the vena cava by heparinized syringe and plasma was obtained by centrifugation. Alanine aminotransferase (ALT/GPT) and aspartate aminotransferase (AST/GOT) activities in the plasma were determined by commercially available test reagents (GPT-UV test Wako and GOT-UV test Wako, respectively; Wako, Osaka, Japan). Normal values were determined using the blood obtained from age-matched, untreated mice. We also confirmed the mice did not show any increase in their plasma ALT and AST following an intravenous injection of a small volume of saline (data not shown).

Isolation and culture of primary hepatocytes

The hepatocytes were isolated by collagenase digestion followed by differential centrifugation according to a previous report [30]. Briefly, at 10 min after intravenous injection of either pCMV-Luc, pEGFP-N1 or pDNA-free saline by the hydrodynamics-based procedure, mice were euthanized and the liver was perfused via the portal vein with preperfusion buffer (Ca^{2+}- and Mg^{2+}-free HEPES buffer, pH 7.2) and then with HEPES buffer (pH 7.5) containing 5 mM $CaCl_2$, 0.005% (w/v) soybean trypsin inhibitor and 0.05% (w/v) collagenase. The liver cells dispersed in ice-cold Hank's-HEPES buffer (pH 7.2) were incubated at 37 °C for 10 min followed by filtration through a Farcon® 100-μm nylon cell strainer (Becton Dickinson, Franklin Lakes, NJ, USA) to remove aggregates of dying cells and then fractionated into hepatocytes and nonparenchymal cells by differential centrifugation. The hepatocytes were suspended in William's medium E supplemented with ITS(+) and penicillin/streptomycin/L-glutamine and seeded on collagen-coated 12-well plates with/without cover slips at a density of 2×10^5 cells/well. After culturing for 24 h at 37 °C, the cells were washed twice with phosphate-buffered saline (PBS) and then fixed with 4% paraformaldehyde for confocal microscopic observation or directly collected by scraping for luciferase assay.

Results

Increase in cell membrane permeability of hepatocytes by the hydrodynamics-based procedure

To examine whether the permeability of the hepatocyte cellular membrane was affected by the hydrodynamics-based procedure, we injected mice intravenously with propidium iodide (PI), a fluorescent substance binding to double-stranded DNA, which is not supposed to cross the plasma membrane of viable cells. Figure 1 shows the liver sections of mice receiving PI by the normal or the hydrodynamics-based procedure. While none of the liver cells were stained with PI following the normal procedure, the hydrodynamics-based procedure caused

an efficient intracellular delivery of PI at 10 min after injection (Figures 1A and 1B). However, a substantial reduction in the fluorescent intensity of nuclear PI staining was observed in a large portion of the hepatocytes at 6 h after the hydrodynamics-based PI injection (data not shown). Simultaneous injection of PI and pEGFP-N1 by the hydrodynamics-based procedure resulted in a significant level of transgene expression without overlap of red and green signals (Figures 1D), indicating that PI-positive cells after a longer period were necrotic or apoptotic with no potentials to express transgene.

To obtain further information on the increased cell membrane permeability of the hepatocytes, we next examined the efflux of GFP from the hepatocytes following the hydrodynamics-based procedure. Because GFP is highly water-soluble and present unbound in the cytosol, it is likely to diffuse from the cytoplasm through the permeable cell membrane. As is evident in Figures 2A and 2B, fluorescent signals of GFP expressed beforehand in the liver were apparently eliminated by the second hydrodynamics-based saline injection. To examine the possibility if the second hydrodynamics-based injection to the same animals might cause significant damage to mouse liver, resulting in the decreased level of GFP, we performed the same experiments using pEGFP-F which encodes a modified form of EGFP that remains bound to the inner face of plasma membrane [27,28]. As a result, the amount of EGFP-F was not significantly affected by the

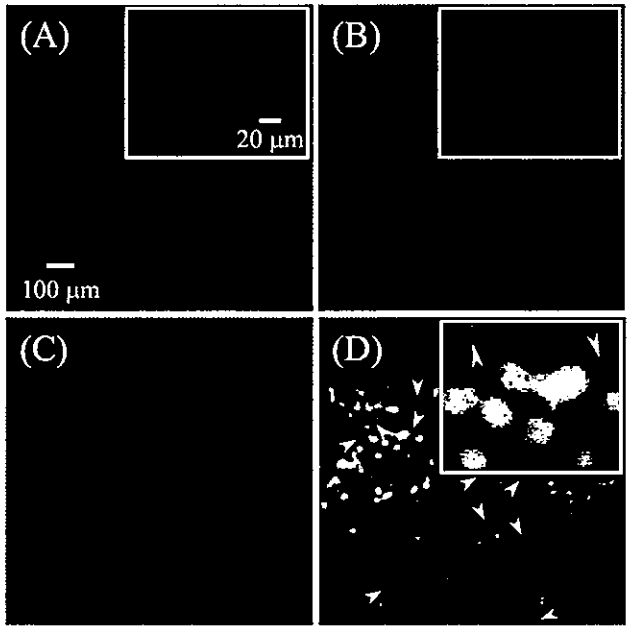

Figure 1. Confocal microscopic images of the liver following an intravenous injection of PI with/without GFP-expressing pDNA. Mice injected with PI (40 μg) by the normal (A) or the hydrodynamics-based (B) procedure were euthanized at 10 min and liver sections were made. Mice that received a simultaneous injection of PI (100 μg) and pEGFP-N1 (25 μg) by the normal (C) or the hydrodynamics-based (D) procedure were euthanized at 6 h and liver sections were made. The images shown are typical of those observed in several visual fields of three mice. Arrowheads indicate the PI-positive cells at 6 h after injection (D). Red: PI; green: GFP

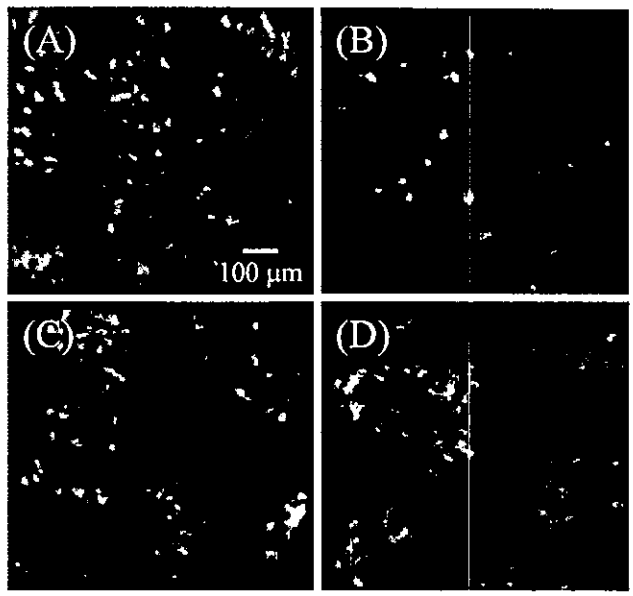

Figure 2. Elimination of pre-expressed GFP in the liver by a large-volume injection of saline. Mice injected beforehand with pEGFP-N1 (25 μg) (A, B) or pEGFP-F (25 μg) (C, D) by the hydrodynamics-based procedure were subjected to a large-volume intravenous injection of saline (1.6 ml) (B, D) or no treatment (A, C) at 6 h. Ten minutes after a pDNA-free saline injection, mice were euthanized and liver sections were made. The images shown are typical of those observed in several visual fields of three mice

second hydrodynamics-based saline injection (Figures 2C and 2D). This was confirmed by an *in vitro* assay where expressed EGFP-F but not EGFP remained within COS-7 cells following membrane permeabilization by Triton X-100 treatment (data not shown). A quantitative analysis by similar experiments using pCMV-Luc, where we did not observe any differences in luciferase activities in the liver between mice with or without the second hydrodynamics-based injection of saline (data not shown), further suggests that the decrease in GFP level is not simply due to a significant damage or denaturation of the expressed GFP. These results further confirm the increased permeability of the hepatocyte cellular membrane.

Time-course of plasma transaminase activities following the hydrodynamics-based procedure

The hepatic enzymes, alanine aminotransferase (ALT) and aspartate aminotransferase (AST), are frequently used as indicators of liver damage. It has been reported that the hydrodynamics-based procedure caused transient liver damage with high serum ALT and AST levels, which rapidly returned to normal in a few days [3,16,31]. We assumed that, similar to the case of GFP effusion shown in Figure 2, the high levels of ALT and AST detected were attributed to release from the hepatocytes when the cellular membrane was transiently rendered permeable by the hydrodynamics-based procedure. Figure 3 shows the plasma concentration profiles of ALT and AST following

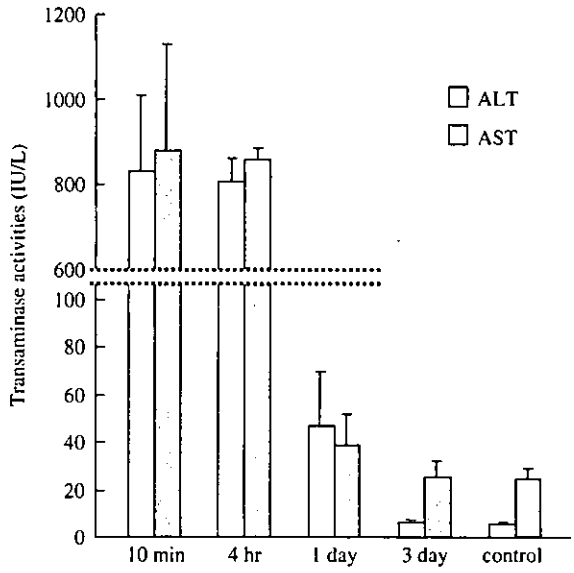

Figure 3. Profiles of plasma transaminase activities following a large-volume injection of saline into mice. Mice received a large-volume intravenous injection of saline (1.6 ml) and blood was collected at the indicated times. Plasma ALT and AST activities were determined. Control represents age-matched, untreated mice. The results are expressed as the mean ± S.D. (n = 3)

a large-volume injection of saline. As expected, the highest values for plasma ALT and AST were detected immediately after injection, i.e. at 10 min, when the large volume of injected saline should dilute the plasma, and, then, these enzyme levels decreased gradually, returning to normal within 3 days (Figure 3). Although it cannot be excluded at this moment that the high levels of ALT and AST observed following the hydrodynamics-based procedure were solely due to cell death, these facts further support the transient increase in the permeability of the hepatocyte cellular membrane.

Competitive effect of excess sham pDNA on transgene expression by the hydrodynamics-based procedure

To discuss the nonspecificity in the process of pDNA cellular uptake following the hydrodynamics-based procedure, we performed a competitive study of transgene expression by a simultaneous injection of pCMV-Luc and an excess of empty vector, pcDNA3. As shown in Figure 4A, transgene expression reached a plateau at 5 μg pCMV-Luc, consistent with the previous report [3]. The transgene expression level in the liver was not affected by simultaneous injection of a saturable amount of pcDNA3 (Figure 4B), suggesting that the hydrodynamics-based gene transfer was a nonspecific process. We also confirmed that the pDNA dose employed in the present study (0.2 μg/mouse) was in the linear region; reduction of the dose caused a substantial fall in transgene expression (Figure 4A).

Duration of the increased membrane permeability following the hydrodynamics-based procedure

To examine how long the hydrodynamics-based procedure maintains the increased permeability of the cell membrane, we performed sequential intravenous injections of a large volume of pDNA-free saline followed by a normal injection of naked pDNA at various time intervals. Figure 5 shows the effect of the time intervals of the two sequential injections on the transgene expression of pCMV-Luc. A prior intravenous injection of a large volume of saline could potentiate a subsequent normal intravenous injection of naked pDNA to produce a significantly high level of luciferase expression in the liver, while no transgene expression was obtained by naked pDNA injection alone in a normal volume (Figure 5). The level of luciferase activity was negatively correlated with the time intervals and marked transgene expression could be obtained up to 15 to 30 min. This phenomenon was also observed in all the other organs tested. Among them, the effect of a prior large-volume injection seemed the most sustained in the lung.

Potential of initially delivered pDNA and RNA for significant transgene expression following the hydrodynamics-based procedure

We examined if a population of intracellular pDNA delivered immediately after injection, during which the increased permeability of the cell membrane appeared to be maintained, could result in a significant level of transgene expression. As shown in Figure 6A, GFP-expressing cells were observed in the hepatocyte culture isolated 10 min after the hydrodynamics-based delivery of pEGFP-N1. Also, a high level of luciferase activity was detected in the cells isolated from mice following the hydrodynamics-based pCMV-Luc injection (Figure 6C). The hepatocytes isolated from saline-treated mice did not show either a GFP signal or luciferase activity (Figures 6B and 6C).

To further provide evidence of the nucleic acid delivered intracellularly immediately after the hydrodynamics-based procedure, we examined the transgene expression at various time points following an intravenous injection of luciferase-expressing RNA. As shown in Figure 7, a significant level of luciferase activity was obtained in the liver as early as 10 min after the hydrodynamics-based procedure. It was confirmed that the produced luciferase activity was derived from the injected RNA not the contaminated template DNA, since RNase A treatment before injection led to a blank level of transgene expression.

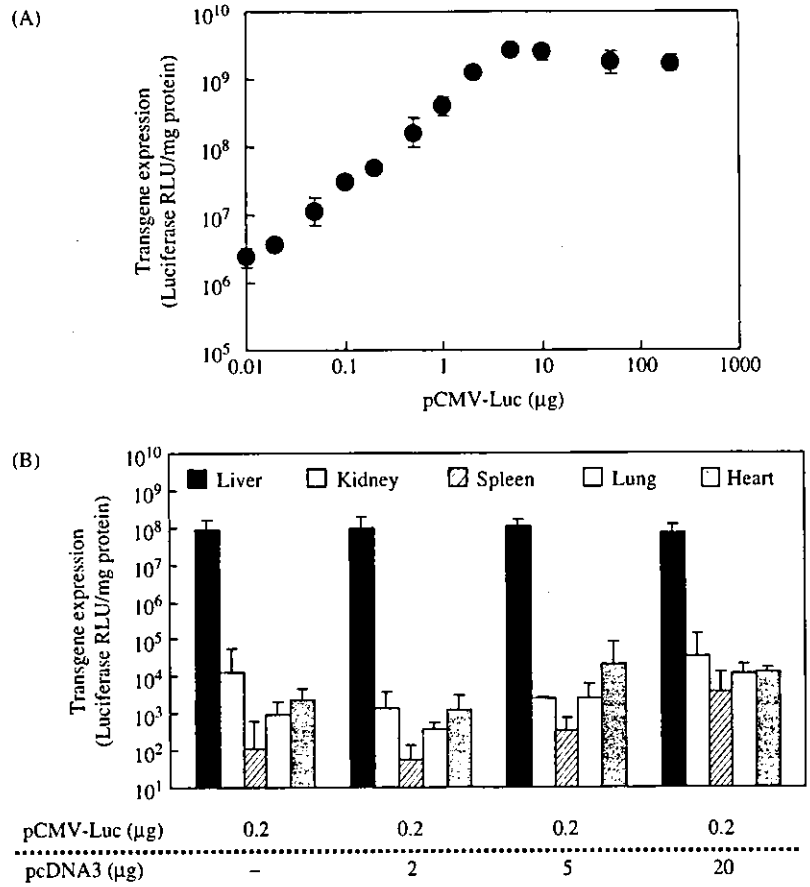

Figure 4. Effect of simultaneous injection of excess sham pDNA on transgene expression by pCMV-Luc following the hydrodynamics-based procedure. Mice received an intravenous injection of various amounts of pCMV-Luc (0.01–200 μg) (A) or a simultaneous injection of pCMV-Luc (0.2 μg) and 10- to 100-fold doses of pcDNA3 (B) by the hydrodynamics-based procedure. At 6 h after injection, mice were euthanized and the luciferase activities in organs were determined. The results are expressed as the mean ± S.D. of at least three mice

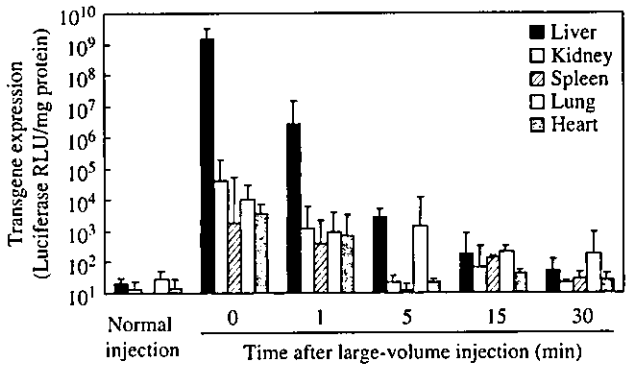

Figure 5. Effect of time interval between a prior large-volume injection of saline and a subsequent normal intravenous injection of pCMV-Luc on transgene expression. Mice received a large-volume intravenous injection of saline (1.6 ml) and, subsequently at the indicated times, an intravenous injection of naked pCMV-Luc (20 μg/mouse) in a normal volume (50 μl). The time interval of 0 min means pCMV-Luc injection by the hydrodynamics-based procedure. The normal injection means a pCMV-Luc injection (20 μg in 50 μl) without any large-volume injection. At 6 h after pDNA injection, mice were euthanized and the luciferase activities in organs were determined. The results are expressed as the mean ± S.D. of at least three mice

Discussion

The hydrodynamics-based gene delivery has been gaining much attention recently and is used very frequently as a simple and convenient efficient *in vivo* transfection method. Following the first reports of the large-volume injection [3,4], Budker *et al.* [25] hypothesized that the cellular uptake mechanism of naked pDNA involved an active, receptor-mediated process. Their hypothesis was prompted mainly by the observations that pDNA administered by the hydrodynamics-based procedure was present around hepatocytes immediately after injection but was internal in hepatocytes at 1 h after injection and that co-injection of excess polyanions inhibited pDNA uptake and expression. In addition, Lecocq *et al.* [32] demonstrated in a subcellular distribution study using differential centrifugation methods that ^{35}S-labeled pDNA remained bound to the outside surface of the plasma membrane for at least 1 h after the hydrodynamics-based procedure, supporting the hypothesis that pDNA was internalized slowly via a specific mechanism. However, in agreement with a notion of a 'hydrodynamics-based' process proposed by Liu and colleagues [3], we have demonstrated that the cellular uptake process

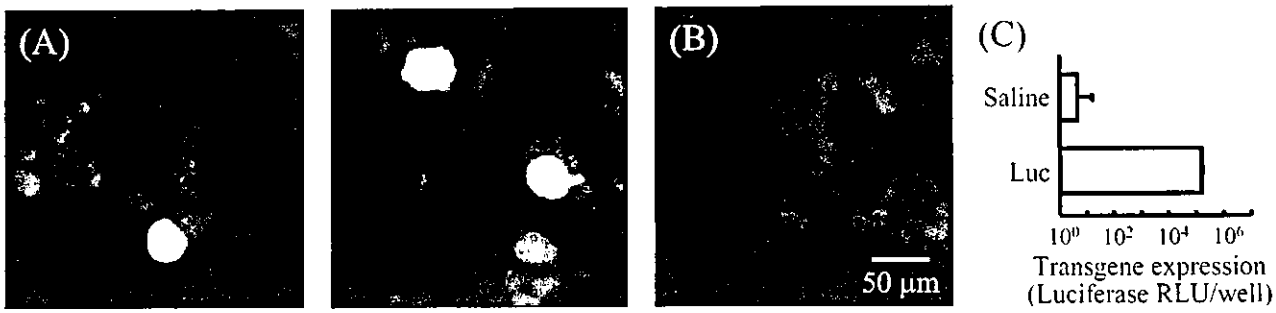

Figure 6. Transgene expression in primary hepatocytes isolated immediately after gene delivery by the hydrodynamics-based procedure. Ten minutes after intravenous injection of either pEGFP-N1 (25 μg), pCMV-Luc (25 μg) or pDNA-free saline by the hydrodynamics-based procedure, mice were euthanized and the hepatocytes were isolated as described in 'Materials and methods'. After 24 h culture, confocal microscopic observation of the cells from pEGFP-N1-injected mice (A) or saline-injected mice (B) was performed and luciferase activities were determined (C). The images shown are typical of those observed in several visual fields. The luciferase activities are expressed as the mean ± S.D. (n = 3)

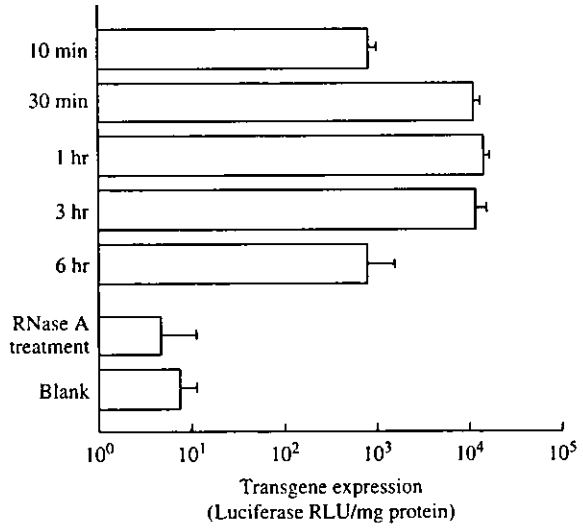

Figure 7. Transgene expression following luciferase-expressing RNA delivery by the hydrodynamics-based procedure. Mice received an intravenous injection of IRES-dependent luciferase-expressing RNA (25 μg) transcribed *in vitro* as described in 'Materials and methods' by the hydrodynamics-based procedure. Mice were euthanized at the indicated time point and the luciferase activities in the liver were determined. For a group of mice, the same RNA (25 μg) was treated with RNase A (15 μg/ml) at 37°C for 15 min before injection. The results are expressed as the mean ± S.D. of three mice

involved in the hydrodynamics-based procedure appears to be nonspecific, since neither the hepatic uptake nor the transgene expression was inhibited by prior administration of polyanions, including poly I, dextran sulfate and heparin [26]. This was supported by the fact that significant hepatic uptake of bovine serum albumin and immunoglobulin G was observed after the hydrodynamics-based procedure [26]. The mechanisms underlying efficient gene transfer by the hydrodynamics-based procedure have not been clarified yet and must be better understood for further applications including gene therapy.

In the present study, we have investigated further the possible mechanisms, which have been controversial so far, governing hydrodynamics-based intracellular gene delivery. PI was effectively incorporated by the liver cells following the hydrodynamics-based procedure (Figure 1B). GFP expressed beforehand and accumulated internally in the cytosol was dramatically eliminated from the hepatocytes following a large-volume injection of saline (Figure 2). These results suggest a facilitated permeation of PI and GFP through the cell membrane, since PI and GFP are not supposed to cross the plasma membrane of viable cells. Contrary to our finding using PI, Budker *et al.* [25] previously observed that injection of a membrane-impermeable dye, TOTO-1, did not lead to nuclear fluorescence in liver cells. This might be accounted for by some differences in the experimental conditions. At least 10% of hepatocytes could be estimated PI-positive at 10 min (Figure 1B). Since Herweijer *et al.* [33] reported that the necrotic areas were less than 1% of the liver following the hydrodynamics-based procedure, all the PI-positive cells observed were not likely to be dead cells. Accordingly, it could be hypothesized that the time-dependent elimination of PI intensity might be a result of efflux or metabolism of PI by viable cells. The fact that only a few cells (estimated approximately 1%) remained PI-positive for a longer period without ability to express GFP further supports this hypothesis. A farnesylated GFP (EGFP-F), a membrane-bound modified form of GFP, was not eliminated by the second large-volume injection of saline (Figures 2C and 2D) and a similar result was obtained in the assay using luciferase (data not shown). While both EGFP and luciferase are supposed cytosolic proteins, the well-known higher water-solubility of EGFP might account for the differences, although the detailed mechanism is unclear. Taken together, it was suggested that the apparent increased permeability of the cell membrane was not simply attributed to cell death or severe cellular damage caused by the invasive nature of the large-volume injection itself.

Nonspecificity in the cellular uptake process of pDNA was further confirmed by a competitive study. A saturable amount of empty vector did not inhibit transgene expression in the liver following the hydrodynamics-based procedure (Figure 4B). In addition, our dose-response study suggests that the transgene expression

was negatively affected if the amount of injected pCMV-Luc exceeded 50 μg/mouse (Figure 4A). This could in part account for the apparent inhibition of transgene expression demonstrated in the report by Budker *et al.* [25], where co-injection of an excess of nonexpressing DNA (500 μg) led to a decrease in reporter gene (pCI-Luc, 50 μg) expression. A prior large-volume injection allowed significant transgene expression by a subsequent naked pDNA injection (Figure 5). The sequential injections at various time intervals revealed that, based on the transgene expression by pCMV-Luc, the effect of the hydrodynamics-based procedure appeared to last more than 15 min and the transient increase in membrane permeability recovered within 30 min.

A significant level of transgene expression was observed in the hepatocyte culture isolated immediately after gene delivery (Figure 6), suggesting that pDNA might be delivered intracellularly with a potential for successful transgene expression following the hydrodynamics-based procedure within the period during which the cell membrane was affected and rendered permeable. However, we cannot yet exclude the possibility that 10 min as perfusion period is sufficient for completion of receptor-mediated internalization of pDNA and that DNA molecules located outside of the cells at the time of isolation would enter the cells afterwards and lead to transgene expression. Hydrodynamics-based injection of luciferase-expressing RNA, which is supposed to proceed translation once delivered intracellularly, resulted in a significant level of transgene expression as early as 10 min after injection (Figure 7). This indicates that intracellular delivery of some RNA has been completed immediately after injection, although a specified period of time appears necessary for completion of mRNA translation. Taken together, although DNA and RNA possess different characteristics such as chemical structure and stability, these results suggest that pDNA might be delivered intracellularly within a short period with a transgene expression potential following the hydrodynamics-based procedure. Therefore, a large portion of the pDNA bound to the outside surface of the plasma membrane for a relatively long time [25,32] might not make a significant contribution to transgene expression. Instead, such pDNA is likely to undergo degradation by accessible external DNase or lysosomal degradation followed by internalization.

We studied the plasma concentration profiles of ALT and AST following the hydrodynamics-based procedure, especially focusing on the earliest phase after injection. As expected from the notion of increased membrane permeability, the highest levels of plasma ALT and AST were observed at 10 min and 4 h (Figure 3). An actual amount of those enzymes detected at 10 min could be higher than that at 4 h, because the blood should be diluted to some extent by the large volume of injected solution immediately after injection. This indicates that the hepatic enzymes ALT and AST immediately diffused out of the hepatocytes following the hydrodynamics-based procedure and were then eliminated gradually from the circulation depending on their pharmacokinetic characteristics, although there should be a possibility that all the observed ALT and AST was simply due to cell death or severe damages caused on some of the hepatocytes that were different from those expressing the transgene. Since ALT and AST are well-known indicators of liver damage, one might think that the values observed in the present study indicate that this procedure is toxic. However, based on the facts that the increased permeability of the cell membrane is only transient and recovered within 30 min, leakage of those enzymes is not totally due to cellular apoptosis or necrosis, but is a transient event caused by the injection procedure. In other words, to accomplish an efficient intracellular delivery of pDNA, an extremely large molecule compared with ALT and AST, it is essential that the hepatocyte cellular membrane is rendered permeable enough to allow transient massive effusion of the hepatic enzymes. The same could apply to the case of gene delivery via electroporation, where the electric pulses open up pores in the cell membranes through which DNA may pass into the interior [34]. From these standpoints, it is conceivable that cellular enzymes such as ALT and AST are not appropriate for the safety evaluation of physical gene delivery strategies including the hydrodynamics-based procedure.

Various nonviral delivery systems have been developed with little success in clinical applications. The delivery system internalized successfully by endocytosis confronts the barrier posed by the endosomal trafficking process which, if not escaped, leads to degradation in lysosomes. This barrier causes a massive drop in the population of therapeutic pDNA molecules, which face up to the following barriers of cytosolic metabolism [35] and nuclear membrane [36,37], diminishing markedly the efficiency of conventional delivery systems. However, it is suggested that the hydrodynamics-based procedure allows direct cytosolic delivery of pDNA through the cell membrane. Thus, pDNA can circumvent the endosomal or lysosomal barriers by this procedure, offering the possibility of a pDNA or pDNA/functional carrier complex aimed at nuclear localization.

In conclusion, we have investigated the possible mechanisms for efficient gene transfer by the hydrodynamics-based procedure and suggested that it would involve in part direct cytosolic delivery of pDNA via an influx along with the large volume of injected solution or a diffusion of pDNA through the cell membrane resulting in transiently increased permeability. In spite of recent advances in vector design, progress in nonviral gene therapy has been unexpectedly delayed mainly because of the inefficiency in delivering genes of interest. Although more studies of safety aspects are required, the marked therapeutic benefit compared with the potential risk of the invasive strategy should encourage the application of the hydrodynamics-based procedure with some modifications and/or the use of suitable devices to become a standard methodology for nonviral gene therapy in the immediate future.

Acknowledgement

This work was supported in part by a Grant-in-Aid for Scientific Research from the Ministry of Education, Culture, Sports, Science and Technology, Japan.

References

1. Nishikawa M, Huang L. Nonviral vectors in the new millennium: delivery barriers in gene transfer. *Hum Gene Ther* 2001; **12**: 861–870.
2. Niidome T, Huang L. Gene therapy progress and prospects: nonviral vectors. *Gene Ther* 2002; **9**: 1647–1652.
3. Liu F, Song Y, Liu D. Hydrodynamics-based transfection in animals by systemic administration of plasmid DNA. *Gene Ther* 1999; **6**: 1258–1266.
4. Zhang G, Budker V, Wolff JA. High levels of foreign gene expression in hepatocytes after tail vein injections of naked plasmid DNA. *Hum Gene Ther* 1999; **10**: 1735–1737.
5. Song YK, Liu F, Zhang G, *et al.* Hydrodynamics-based transfection: simple and efficient method for introducing and expressing transgenes in animals by intravenous injection of DNA. *Methods Enzymol* 2002; **346**: 92–105.
6. Kobayashi N, Kuramoto T, Chen S, *et al.* Therapeutic effect of intravenous interferon gene delivery with naked plasmid DNA in murine metastasis models. *Mol Ther* 2002; **6**: 737–744.
7. Kobayashi N, Matsui Y, Kawase A, *et al.* Vector-based in vivo RNA interference: dose- and time-dependent suppression of transgene expression. *J Pharmacol Exp Ther* 2004; **308**: 688–693.
8. Kobayashi N, Hirata K, Chen S, *et al.* Hepatic delivery of particulates in the submicron range by a hydrodynamics-based procedure: implications for particulate gene delivery systems. *J Gene Med* 2004; in press.
9. Wu X, He Y, Falo LD Jr, *et al.* Regression of human mammary adenocarcinoma by systemic administration of a recombinant gene encoding the hFlex-TRAIL fusion protein. *Mol Ther* 2001; **3**: 368–374.
10. Wang Z, Qiu SJ, Ye SL, *et al.* Combined IL-12 and GM-CSF gene therapy for murine hepatocellular carcinoma. *Cancer Gene Ther* 2001; **8**: 751–758.
11. Chang J, Sigal LJ, Lerro A, *et al.* Replication of the human hepatitis delta virus genome is initiated in mouse hepatocytes following intravenous injection of naked DNA or RNA sequences. *J Virol* 2001; **75**: 3469–3473.
12. He Y, Pimenov AA, Nayak JV, *et al.* Intravenous injection of naked DNA encoding secreted flt3 ligand dramatically increases the number of dendritic cells and natural killer cells in vivo. *Hum Gene Ther* 2000; **11**: 547–554.
13. Zhang G, Song YK, Liu D. Long-term expression of human alpha1-antitrypsin gene in mouse liver achieved by intravenous administration of plasmid DNA using a hydrodynamics-based procedure. *Gene Ther* 2000; **7**: 1344–1349.
14. Maruyama H, Higuchi N, Nishikawa Y, *et al.* High-level expression of naked DNA delivered to rat liver via tail vein injection. *J Gene Med* 2002; **4**: 333–341.
15. Yang J, Chen S, Huang L, *et al.* Sustained expression of naked plasmid DNA encoding hepatocyte growth factor in mice promotes liver and overall body growth. *Hepatology* 2001; **33**: 848–859.
16. Miao CH, Thompson AR, Loeb K, *et al.* Long-term and therapeutic-level hepatic gene expression of human factor IX after naked plasmid transfer in vivo. *Mol Ther* 2001; **3**: 947–957.
17. Yang J, Dai C, Liu Y. Systemic administration of naked plasmid encoding hepatocyte growth factor ameliorates chronic renal fibrosis in mice. *Gene Ther* 2001; **8**: 1470–1479.
18. Budker V, Zhang G, Knechtle S, *et al.* Naked DNA delivered intraportally expresses efficiently in hepatocytes. *Gene Ther* 1996; **3**: 593–598.
19. Zhang G, Vargo D, Budker V, *et al.* Expression of naked plasmid DNA injected into the afferent and efferent vessels of rodent and dog livers. *Hum Gene Ther* 1997; **8**: 1763–1772.
20. Zhang G, Budker V, Williams P, *et al.* Efficient expression of naked DNA delivered intraarterially to limb muscles of nonhuman primates. *Hum Gene Ther* 2001; **12**: 427–438.
21. Budker V, Zhang G, Danko I, *et al.* The efficient expression of intravascularly delivered DNA in rat muscle. *Gene Ther* 1998; **5**: 272–276.
22. Maruyama H, Higuchi N, Nishikawa Y, *et al.* Kidney-targeted naked DNA transfer by retrograde renal vein injection in rats. *Hum Gene Ther* 2002; **13**: 455–468.
23. Zhang G, Budker V, Williams P, *et al.* Surgical procedures for intravascular delivery of plasmid DNA to organs. *Methods Enzymol* 2002; **346**: 125–133.
24. Eastman SJ, Baskin KM, Hodges BL, *et al.* Development of catheter-based procedures for transducing the isolated rabbit liver with plasmid DNA. *Hum Gene Ther* 2002; **13**: 2065–2077.
25. Budker V, Budker T, Zhang G, *et al.* Hypothesis: naked plasmid DNA is taken up by cells in vivo by a receptor-mediated process. *J Gene Med* 2000; **2**: 76–88.
26. Kobayashi N, Kuramoto T, Yamaoka K, *et al.* Hepatic uptake and gene expression mechanisms following intravenous administration of plasmid DNA by conventional and hydrodynamics-based procedures. *J Pharmacol Exp Ther* 2001; **297**: 853–860.
27. Aronheim A, Engelberg D, Li N, *et al.* Membrane targeting of the nucleotide exchange factor Sos is sufficient for activating the Ras signaling pathway. *Cell* 1994; **78**: 949–961.
28. Hancock JF, Cadwallader K, Marshall CJ. Methylation and proteolysis are essential for efficient membrane binding of prenylated p21K-ras(B). *EMBO J* 1991; **10**: 641–646.
29. Nomura T, Yasuda K, Yamada T, *et al.* Gene expression and antitumor effects following direct interferon (IFN)-gamma gene transfer with naked plasmid DNA and DC-chol liposome complexes in mice. *Gene Ther* 1999; **6**: 121–129.
30. Nishikawa M, Takemura S, Takakura Y, *et al.* Targeted delivery of plasmid DNA to hepatocytes in vivo: optimization of the pharmacokinetics of plasmid DNA/galactosylated poly(L-lysine) complexes by controlling their physicochemical properties. *J Pharmacol Exp Ther* 1998; **287**: 408–415.
31. Rossmanith W, Chabicovsky M, Herkner K, *et al.* Cellular gene dose and kinetics of gene expression in mouse livers transfected by high-volume tail-vein injection of naked DNA. *DNA Cell Biol* 2002; **21**: 847–853.
32. Lecocq M, Andrianaivo F, Warnier MT, *et al.* Uptake by mouse liver and intracellular fate of plasmid DNA after a rapid tail vein injection of a small or a large volume. *J Gene Med* 2003; **5**: 142–156.
33. Herweijer H, Zhang G, Subbotin VM, *et al.* Time course of gene expression after plasmid DNA gene transfer to the liver. *J Gene Med* 2001; **3**: 280–291.
34. Somiari S, Glasspool-Malone J, Drabick JJ, *et al.* Theory and in vivo application of electroporative gene delivery. *Mol Ther* 2000; **2**: 178–187.
35. Lechardeur D, Sohn KJ, Haardt M, *et al.* Metabolic instability of plasmid DNA in the cytosol: a potential barrier to gene transfer. *Gene Ther* 1999; **6**: 482–497.
36. Wilke M, Fortunati E, van den Broek M, *et al.* Efficacy of a peptide-based gene delivery system depends on mitotic activity. *Gene Ther* 1996; **3**: 1133–1142.
37. Zabner J, Fasbender AJ, Moninger T, *et al.* Cellular and molecular barriers to gene transfer by a cationic lipid. *J Biol Chem* 1995; **270**: 18 997–19 007.